Technologia i Automatyzacja Montażu
Assembly Techniques and Technologies

TiAM
Technologia i Automatyzacja Montażu

Open Access: journals.prz.edu.pl/tiam • e-ISSN-2450-8217 • Volume 123, Issue 1, 2024

Publisher: Łukasiewicz Research Network – Warsaw Institute of Technology • Rzeszow University of Technology • Patronage SIMP • Since 1993

RZESZOW UNIVERSITY OF TECHNOLOGY

Łukasiewicz
Warsaw Institute of Technology

TiAM
Technologia i Automatyzacja Montażu

CONTENTS

3
Konrad Jamróz, Lidia Gałda
The effect of selected WEDM parameters on cut surface quality of 2017A aluminum
Wpływ wybranych parametrów elektrodrążenia na jakość powierzchni cięcia aluminium 2017A

10
Camelia Avram, Laura-Flavia Păcurar, Dan Radu
Sign Language Classifier based on Machine Learning
Klasyfikator języka migowego oparty na uczeniu maszynowym

16
Jozef Husár, Stella Hrehova, Piotr Trojanowski, Markus Brillinger
Optimizing the Simulation of Conveyor Systems through Digital Shadow Integration to Increase Assembly Efficiency
Optymalizacja symulacji systemów przenośników poprzez integrację cyfrowego cienia dla zwiększenia wydajności montażu

23
Witold Habrat, Jarosław Tymczyszyn, Anna Skroban, Nikolaos Karkalos
Effect of TiBW Anti-Wear Coating on Cutting Tools for Milling of Nickel Alloys on Tool Wear and Integrity of State of The Technological Surface Layer
Wpływ powłoki przeciwzużyciowej TiBW na frezach do obróbki stopów niklu na zużycie narzędzia oraz stan technologicznej warstwy wierzchniej

30
Pierluigi Rea, Erika Ottaviano, Lucia Figuli
Simulation based study of Ground Mobile Robots for Inspection and Control of the Bridge Assembly Process
Badanie oparte na symulacji naziemnych robotów mobilnych do inspekcji i kontroli procesu montażu mostu

37
Andrzej Chmielowiec, Karol Łysiak, Jindřich Viliš
Development of a Basic CAM Processor for a Collaborative Robot for Workshop Automation
Opracowanie podstawowego procesora CAM dla robota współpracującego na potrzeby automatyzacji prac warsztatowych

Quarterly „Technologia i Automatyzacja Montażu" is listed on the list of scored journals of Polish Ministry of Education and Science - 40 points.

Technologia i Automatyzacja Montażu

Volume 123, Issue 1/2024, Pages 3-9
https://doi.org/10.7862/tiam.2024.1.1

Original Research

THE EFFECT OF SELECTED WEDM PARAMETERS ON CUT SURFACE QUALITY OF 2017A ALUMINUM

WPŁYW WYBRANYCH PARAMETRÓW ELEKTRODRĄŻENIA NA JAKOŚĆ POWIERZCHNI CIĘCIA ALUMINIUM 2017A

Konrad JAMRÓZ[1], Lidia GAŁDA[1,*]

[1] Department of Machines Technology and Production Engineering, Faculty of Mechanical Engineering and Aeronautics, Rzeszow University of Technology, Powstańców Warszawy 12, 35-959 Rzeszów, Poland

* Corresponding author: lgktmiop@prz.edu.pl

Abstract

With the wire electrical discharge machining (WEDM), good quality machined surfaces can be achieved. The WEDM is worth considering for machining fasteners used in assembly processes. This paper presents a study of the WEDM cutting process of aluminum 2017A using an WEDM machine of the FR 400 type. After applying different cutting speeds, the characteristics of the cut surface were evaluated. Despite some differences in the shape of surface profiles and surface morphology noted after WEDM cutting at different speeds, the analysis of variance concluded that the WEDM cutting speed in the studied variation range of 23-125 µm/s has no significant effect on surface roughness. At the highest speed studied, machining efficiency can be increased, affecting cost and energy reduction, while maintaining an acceptable and comparable level of surface quality after WEDM cutting.

Keywords: aluminum 2017A, fasteners for assembly, WEDM, surface characteristics, analysis of variance

Streszczenie

Dzięki obróbce elektroerozyjnej można uzyskać dobrą jakość obrabianych powierzchni. Warto rozważyć zastosowanie obróbki elektroerozyjnej do obróbki elementów złącznych wykorzystywanych w procesach montażowych. W artykule przedstawiono badania procesu cięcia elektroerozyjnego aluminium 2017A z zastosowaniem elektrodrążarki typ FR 400. Po zastosowaniu zróżnicowanej prędkości obróbki poddano ocenie stan powierzchni cięcia. Pomimo zauważonych pewnych różnic w kształcie profili powierzchni i morfologii powierzchni po cięciu elektroerozyjnym z różnymi prędkościami, to w wyniku analizy wariancji stwierdzono, że prędkość cięcia poprzez elektrodrążenie w badanym zakresie zmienności 23-125 µm/s nie wywiera istotnego wpływu na chropowatość powierzchni. Przy największej badanej prędkości można zwiększyć wydajność obróbki, wpływając na zmniejszenie kosztów i energii, zachowując akceptowalny i porównywalny poziom jakości powierzchni po cięciu elektroerozyjnym.

Słowa kluczowe: aluminium 2017A, elementy złączne w montażu, obróbka elektrodrążeniem, stan powierzchni, analiza wariancji

1. Introduction

Automation of the assembly process specifically requires high quality components from which a machine unit or finished product is assembled. Analyzing the assembly process, it can be concluded that individual operations do not affect the properties of the assembled part in the same way. Taking into account the design of the assembled part or assembly, among other things, the quality of the fasteners connecting the individual parts of the structure is very important. The quality of fasteners should be understood as such features as the type of materials and its properties, as well as the design and finish. One

This is an Open Access article distributed under the terms of the Creative Commons Attribution License CC BY 4.0 (https://creativecommons.org/licenses/by/4.0/)

of the materials used for fasteners is aluminum type 2017A, which, due to the addition of copper and magnesium, is characterized by relatively high hardness and high strength (Kuczmaszewski et al., 2015; Skrzypek, 2019). As previously mentioned, the reliability of the assembly will be affected by the way the fasteners are finished, since technological processing has a significant impact on the quality of the surface layer. One of the first operations that is performed after supplying suitable material is the cutting operation. There are many cutting methods from traditional saw cutting to laser or water jet cutting. One of the more interesting cutting techniques is electro-discharge cutting, which makes it possible to realize machining of parts with complex shapes requiring high dimensional accuracy. It is considered the most precise cutting method, but to achieve the required dimensional accuracy and surface quality, several machining passes must be made along the cutting profile (Ho et al, 2004). The WEDM is most often used for machining tempered steels, tool steels, carbides or other materials usually of high hardness, but due to the advantages of WEDM such as high precision and good surface quality after machining, it is worth considering its application for machining other materials.

In the WEDM cutting process, the area between the wire electrode and the workpiece is subjected to thermal effects that cause overmelting and burning of the material, resulting in changes in the structure and surface properties of the cut workpiece. Three characteristic layers can be distinguished in the microstructure of the surface layer after WEDM (Mazurkiewicz, 2010; Oniszczuk et al. 2015):

- the first is the so-called white layer - it is formed on the surface of the material due to the solidification of previously melted metal that has not been removed from the cutting gap;
- the next layer, located directly below the white layer, is the thermal influence layer;
- the third layer is the so-called tempered layer.

Tensile stresses are present in the surface layer after the WEDM process, resulting from the shrinkage of the heated material. The value of the stresses is determined by the energy and duration of individual electrical discharges. The presence of stresses in the surface layer can contribute to the formation of microstructure defects in the form of craters and micro-cracks (Mazurkiewicz, 2010). The geometric structure of the surface after the WEDM cutting process is random in nature with a significant density of surface profile elements (Oniszczuk et al. 2015).

In the WEDM cutting process, a number of process variables can be distinguished that affect machining performance, electrode wear, thickness of the heat affected layer, surface roughness and changes in the structure of the material being cut. These factors are related to the energy conditions of the process, the chemical composition and properties of the dielectric, working electrode, workpiece material, stiffness and parameters of the cutting machine, among others (Mazurkiewicz, 2010).

This paper presents the results of a study on the WEDM cutting of 2017A aluminum, especially on the effect of cutting speed on the cut surface quality. The WEDM cutting is typical to process hard material but considering the capabilities of the process, possible advantages in cutting a relatively soft material such as aluminum were investigated.

2. Research methodology

In the article the process of cutting aluminum 2017A by wire electrical discharge machining is examined. Aluminum 2017A belongs to a group of aluminum-copper-magnesium alloys called duralumin or copper durals. The heat treatment of this alloy mainly consists of precipitation hardening, which includes supersaturation and aging processes (Kuczmaszewski et al., 2015; Skrzypek, 2019). The chemical composition of aluminum 2017A is given in Table 1.

Table 1. Chemical composition of aluminum 2017A (http, 2024; PN-EN, 2022-11)

Si (%)	Fe (%)	Cu (%)	Mn (%)	Mg (%)
0,20-0,80	≤ 0,70	3,50-4,50	0,40-1,0	0,40-1,0
Cr (%)	**Zn (%)**	**Zr+Ti (%)**	**others (%)**	**Al (%)**
≤ 0,10	≤ 0,25	≤ 0,25	≤ 0,15	rest

Table 2 shows the properties of aluminum 2017A. Aluminum 2017A is used for die forging or cast parts, mainly in the aerospace, automotive, engineering and construction industries. Parts made from this alloy can operate not only at ambient temperatures, but also at higher temperatures, due to increased heat resistance caused by the addition of manganese, among other things.

Table 2. Selected properties of aluminum 2017A (Kuczmaszewski et al., 2015; http, 2024)

Hardness after supersaturation and natural aging	110 HB
Hardness after annealing	55 HB
Supersaturation temperature	490-510ºC
Aging temperature	170-190ºC
Density	2,8 g/cm^3
Coefficient of linear expansion	$23 \cdot 10^{-6}$ K^{-1} (20ºC)

Since aluminum 2017A is characterized by relatively high hardness and high strength (Kuczmaszewski et al., 2015; Skrzypek, 2019), it is also used for fasteners.

The process of cutting the 2017A material was carried out using the FR 400 numerically controlled WEDM cutting machine. Molybdenum wire with a diameter of 0.18 mm was used as the electrode. The dielectric fluid was deionized water. Fig. 1 shows photos of the FR 400 WEDM cutter.

Fig. 1. Photos of the FR 400 machine (Jamróz, 2022)

According to the machine specification (manual, 2021), the roughness parameter Ra after one machining pass should be less than or equal to 2 µm, while after several passes Ra should be less than or equal to 0.8 µm.

An aluminum cube of material was subjected to WEDM cutting at four different speeds. A so-called single machining pass of the WEDM cut was performed. A photo of the cut material is shown in Fig. 2.

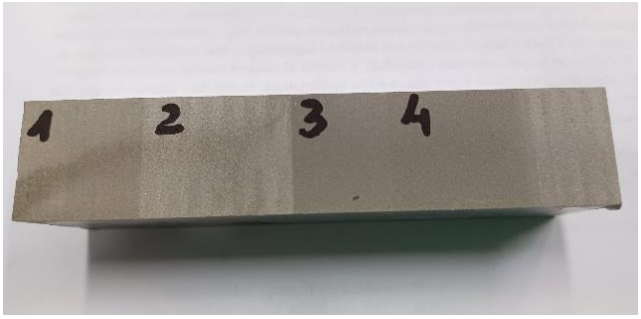

Fig. 2. Photo of aluminum 2017A after WEDM cutting

In the experimental study, a variable cutting speeds [µm/s] were adopted. The current I [A] was automatically changed based on the cutting speed setting.

Electrical discharge cutting was performed with a single pass. The surface after cutting is usually subjected to subsequent machining operations, since the obtained surface roughness parameters are not, as far as values are concerned, equal to those expected for the finished product. However, too high values of surface roughness after WEDM cutting can affect the subsequent machining process and prolong the production process, or increase production costs by requiring additional machining operations. Therefore, the selection of appropriate process parameters of the implemented operations becomes so important.

A statistical method with one-factor analysis of variance was used to quantitatively assess the significance of the selected technological parameter effect. More details about the method and the example of application are presented in (Gałda et al., 2022). The input factor was the cutting speed at four levels of variation in the range of 23 - 125 µm/s (Table 3).

Table 3. The WEDM cutting process parameters

Cutting surface (fig. 2)	Aluminum 2017A	
	Cutting speed [µm/s]	Current I [A]
1	60	2
2	125	3
3	35	1÷2
4	23	1

The output factors were the selected surface roughness parameters after WEDM cutting. A significance level of $\alpha = 0.05$ was adopted.

Surface roughness was measured using a Surtronic 25 stylus profilometer, while selected surface roughness parameters were calculated using TalyProfile Lite 6 software. Measurements of each cut surface were performed with three times repetition on a measuring section of 8 mm. Mainly the amplitude parameters (Rp, Rv, Ra) were analyzed, but given the presence of characteristic paths on the cut samples, the longitudinal parameter RSm was also analyzed.

A Phenom Pro scanning electron microscope was used to observe the surface of the samples after WEDM cutting. The SEM images of the surfaces after WEDM cutting were taken at 510x magnification.

3. Results and their analysis

Figure 3 shows selected representative primary profiles of the surface after WEDM cutting at varying speeds. The results of the measurements of selected roughness parameters are shown in Table 4. Analyzing the surface profiles, it can be seen that they are all characterized by significant surface irregularities with sharply ended steep peaks and depressions.

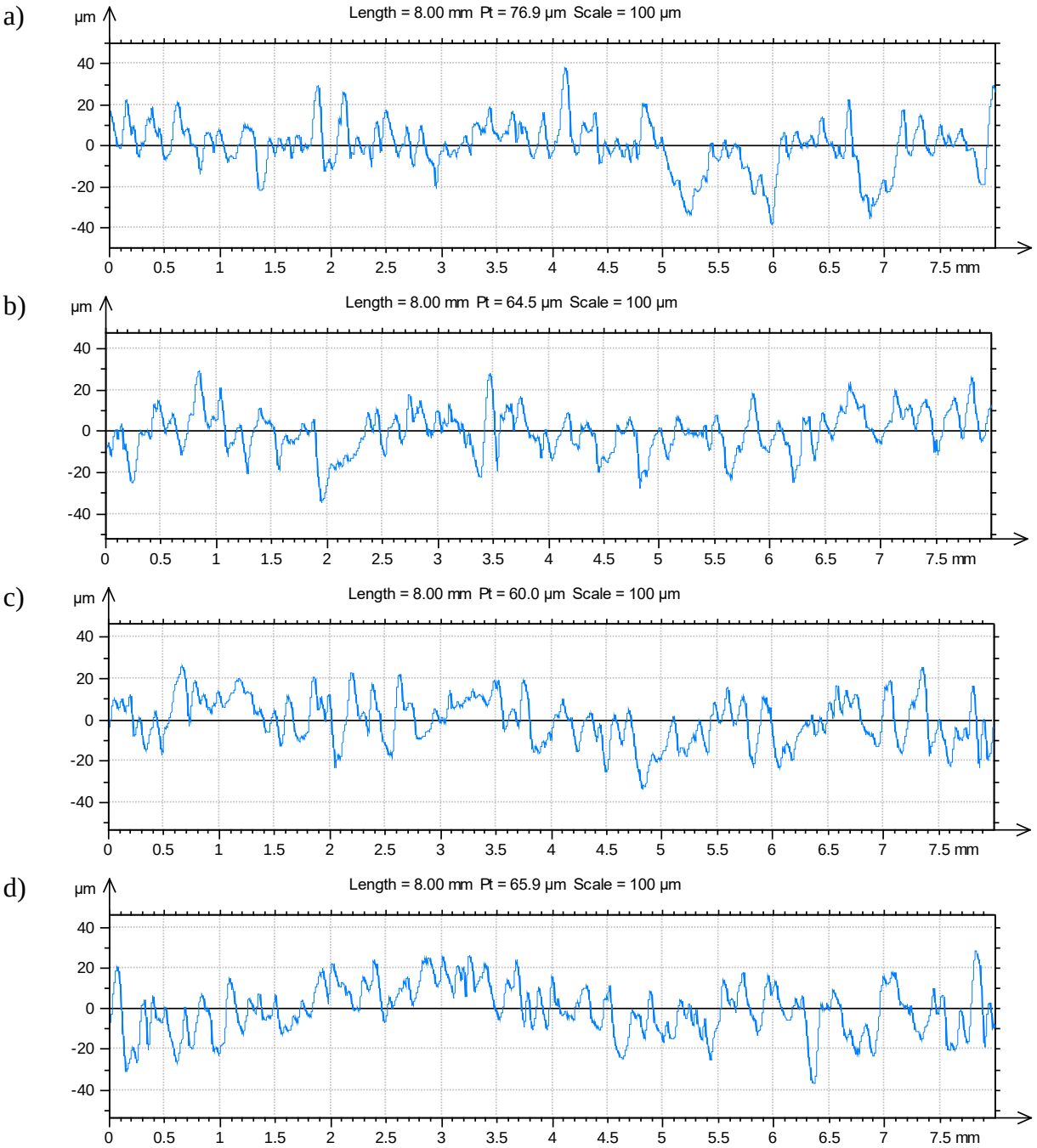

Fig. 3. Selected surface profiles after WEDM cutting with different speeds: 23 µm/s (a), 35 µm/s (b), 60 µm/s (c), 125 µm/s (d)

On the surface profiles (Fig. 3 a, b) after WEDM cutting at lower speeds the valleys of greater width randomly appear than those found on the compared surface profiles (Fig. 3 c, d), where the cutting speed was several times higher. Comparing selected amplitude parameters of surface roughness, it can be concluded that with increasing cutting speed in most cases their value increases (Table 4).

The average value of the Ra parameter, which presents the average deviation of the profile from the mean line (PN-EN ISO, 2022-06), increases by about 18% as the cutting speed increases. The increase in Ra is mainly due to an increase in the value of the maximum depressions in the profile of the Rv surface (increase of about 16.7%) as the cutting speed increases. The parameter Rp, which determines the highest peak of the profile, increased in value by about 0.7% with increased WEDM cutting speed. The distances between the elements of the profile were also examined, as characteristic paths of varying width were observed on the cutting surfaces. The values of the longitudinal roughness parameter RSm changed

with the change in cutting speed, but no significant correlations between these parameters were noted.

Table 4. Measured values of selected parameters of surface profiles after WEDM with average and standard deviation values

Cutting speed [µm/s]	Surface roughness parameters			
	Ra [µm]	Rp [µm]	Rv [µm]	RSm [mm]
23	6,43	17,1	16,6	0,193
	5,74	15,8	15,9	0,196
	6,33	20,8	17,5	0,18
average	**6,167**	**17,9**	**16,7**	**0,19**
standard deviation	0,37	2,59	0,80	0,01
35	6,37	18,5	18,9	0,178
	5,89	18	14	0,16
	6,25	17	18,2	0,218
average	**6,17**	**17,83**	**17,03**	**0,185**
standard deviation	0,25	0,76	2,65	0,03
60	6,93	17,7	17,1	0,189
	7,69	17,6	22,2	0,202
	7,25	19,9	18,8	0,211
average	**7,29**	**18,4**	**19,37**	**0,201**
standard deviation	0,38	1,30	2,60	0,01
125	6,91	15,9	17	0,194
	7,45	18,3	19,8	0,19
	7,54	19,9	21,7	0,18
average	**7,3**	**18,03**	**19,5**	**0,188**
standard deviation	0,34	2,01	2,36	0,01

Analyzing the results, it was noted that the dimensions of the standard deviation from the mean value of the parameters Rp and Rv, as well as RSm, are relatively large when compared to the dimension of the change in the values of these parameters when the cutting speed is changed (fig. 4 b-d). Only the standard deviation from the mean value of the Ra parameter is relatively small compared to the change in Ra values (Fig. 4a), characterizing the surface profiles after WEDM cutting at different speeds. Here it should be noted that the Ra parameter is a parameter, presenting the average of many measured points, so some important relationships may be lost (unnoticed). In such a situation, it is worth checking whether the studied technological parameter (WEDM cutting speed) significantly affects the selected output factors, using statistical methods. In order to assess whether the difference in the value of roughness parameters at different cutting speeds is significant, a one-way analysis of variance of the obtained surface roughness results was applied.

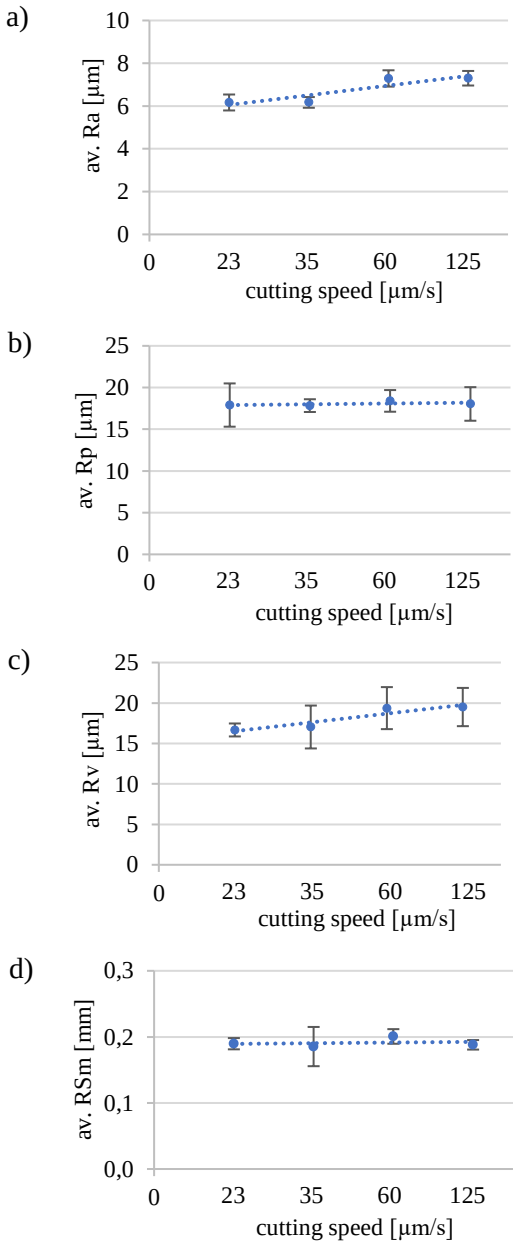

Fig. 4. Average values of Ra (a), Rp (b), Rv (c) and RSm (d) surface roughness parameters versus increasing the cutting speed

The SEM images show some differences in the surface morphology after WEDM cutting. In general, the morphology of the surface after WEDM cutting is characterized by the presence of randomly distributed craters formed by electrical discharges and microcracks formed when the heated material shrinks (Fig. 5). The surfaces cut at lower speeds (Fig. 5 a, b) show craters with irregular shapes and much larger dimensions compared to those observed on surfaces cut at higher speeds (Fig. 5 c, d). The results of the surface morphology observations correlate with the wider valleys observed on the surface profiles when lower cutting speeds were used.

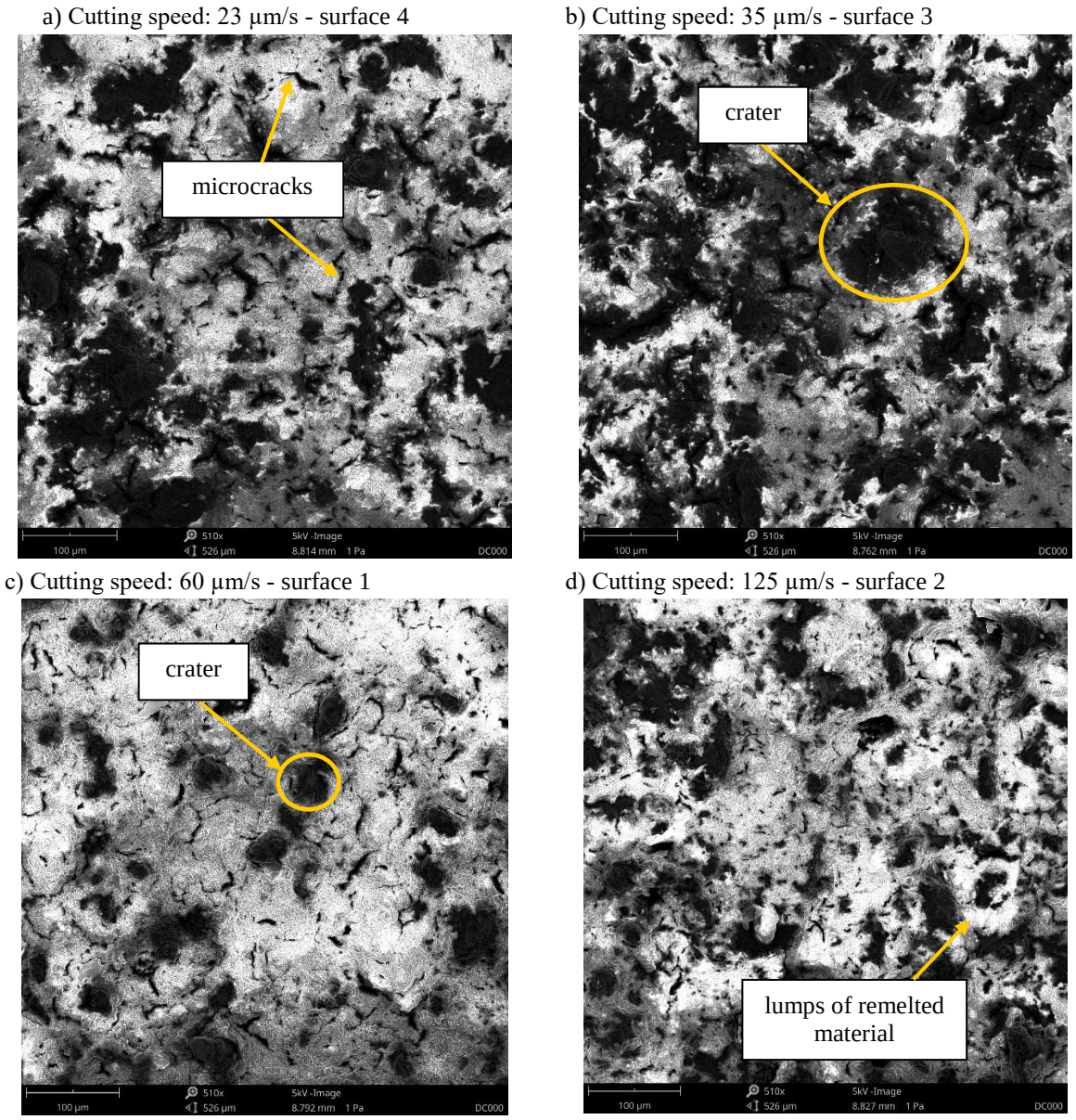

Fig. 5. The SEM images of cutting surfaces with different speeds in the range of 23 µm/s to 125 µm/s (a-d)

In the case of surfaces cut at higher speeds (Fig. 5 c, d), i.e. at the same time at higher current intensity, lumps of remelted material, characteristic of surfaces remelted by thermal interaction, are clearly visible.

Analyzing the variance, it is necessary to assume the null hypothesis H_0, stating that there is no significant effect of cutting speed on the studied surface roughness parameters, i.e. Ra, Rp, Rv and RSm. For each of the analyzed output factors, the analysis is carried out separately. A significance level of α equal to 0.05 was assumed in the study. As a result of the calculations, empirical values of the F index were obtained, which were compared with the critical value of the F_{cr} index, read from the Fisher-Snedecor statistical table. Table 5 shows the results of the one-way analysis of variance for the four selected surface roughness parameters.

Table 5. One factor (cutting speed) variance analysis for surface roughness parameters: Ra, Rp, Rv and RSm

Output parameter	F	F_{cr}	p-value
Ra	10,96	4,07	0,003
Rp	0,06		0,980
Rv	1,35		0,325
RSm	0,48		0,703

In the case of roughness parameters Rp, Rv and RSm, the null hypothesis H_0 of no significant effect of WEDM cutting speed was confirmed. This means that regardless of the change in the value of the

technological parameter: cutting speed in the range of 23 µm/s to 125 µm/s, the change in the mentioned roughness parameters is not statistically significant. Only in the case of the Ra parameter the statistical significance of the effect of the cutting speed parameter was shown. However, it should be noted here that the Ra parameter is characterized by the fact that it is determined based on the average of many points, so the analysis based on the variance may be inadequate in this case. Taking into account the obtained results, it should be concluded that the cutting speed of the tested 2017A aluminum material in the range of 23-125 µm/s has no significant effect on the selected surface roughness parameters. Therefore, it is possible to consider increasing the production efficiency by increasing the cutting speed of the WEDM method. Figure 6 presents the cutting length of the 2017A aluminum material of the thickness presented in the article, assuming cutting for 8 hours without interruption.

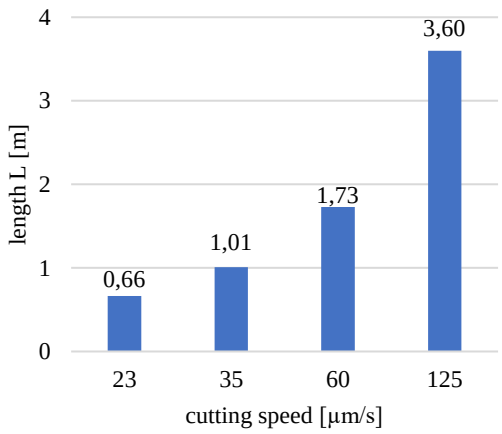

Fig. 6. Length of material that can be cut in one 8-hour shift at different WEDM cutting speeds

With a more than fivefold increase in cutting speed from 23 µm/s to 125 µm/s, a more than fivefold increase in productivity was obtained, which is quite obvious. On the other hand, it is worth noting the savings from reduced energy consumption, since the current is increased only three times from 1 A to 3 A, so in addition to the reduction in machining time, measurable financial savings are also gained. In times of fierce competition in the market, such factors as increased productivity, reduced machining time and energy savings, while ensuring the quality of the product at the appropriate level, gives an advantage over the competitors.

4. Conclusions

Observation of surface profiles and SEM surface images revealed that at low WEDM cutting speeds there are randomly distributed craters with irregular shapes and relatively large dimensions. At higher WEDM cutting speeds, surface irregularities are characterized by a slightly greater maximum depth and there are lumps of remelted material on the surface.

As a result of the analysis of variance of the values of selected surface roughness parameters of aluminum 2017A after WEDM cutting at different cutting speeds, it was found that the cutting speed in the range of 23-125 µm/s has no significant effect on the surface roughness parameters Rp, Rv, RSm.

Since the surface quality determined by the roughness parameters after WEDM cutting does not depend on the cutting speed in the studied range, so there is a possibility to increase productivity, reduce machining time and save energy when realizing WEDM cutting of aluminum 2017A with the highest speed equal to 125 µm/s.

References

Gałda L., Pająk D. (2022). Analysis of the application of SiC ceramics as a tool material in the slide burnishing process. Technologia i Automatyzacja Montażu, vol. 1, 45-57. DOI: 10.7862/tiam.2022.1.5.

Ho K.H., Newman S.T., Rahimifard S., Allen R.D. (2004). State of the art in wire electrical discharge machining (WEDM). International Journal of Machine Tools and Manufacture, vol. 44, No. 12-13, 1247-1259. http://dx.doi.org/10.1016/j.ijmachtools.2004.04.017.

Instruction manual for the FR 400 machine tool (2021).

Jamróz K. (2022). Analysis of the influence of WEDM parameters on the surface quality. Diploma thesis, Rzeszów.

Kuczmaszewski J., Zaleski K. (2015). Machining of aluminum and magnesium alloys. Lublin University of Technology, Lublin.

Mazurkiewicz A. (2010). Factors influencing the quality of production using electro-discharge technology. Logistyka, no. 6.

Oniszczuk-Świercz D., Świercz R. (2015). Influence of processing parameters on the state of the surface layer after WEDM process. Mechanik, no. 1, 14-17.

Skrzypek S. J., Przybyłowicz K. (2019). Metal engineering and material technologies. Wydawnictwo Naukowo-Techniczne, Warsaw.

PN-EN 573-3+A1:2022-11, Aluminum and aluminum alloys - Chemical composition and form of wrought products - Part 3: Chemical composition and form of products.

PN-EN ISO 21920-2:2022-06, Geometrical product specifications (GPS) - Surface texture: Profile - Part 2: Terms, definitions and surface texture parameters.

http://www.steelnumber.com/en/steel_alloy_composition_eu.php?name_id=1035 (access 27.02.2024).

Technologia i Automatyzacja Montażu

Volume 123, Issue 1/2024, Pages 10-15
https://doi.org/10.7862/tiam.2024.1.2

Original Research

SIGN LANGUAGE CLASSIFIER BASED ON MACHINE LEARNING

KLASYFIKATOR JĘZYKA MIGOWEGO OPARTY NA UCZENIU MASZYNOWYM

Camelia AVRAM[1,*], Laura-Flavia PĂCURAR[1], Dan RADU[1]

[1] Department of Automation, Technical University of Cluj Napoca, Ge. Bariţiu 26-28, Cluj-Napoca, Romania

* Corresponding author: camelia.avram@aut.utcluj.ro, tel.: 0040 264 401 822

Abstract

Sign language represents an efficient way for individuals with hearing impairments to communicate. We propose a sign recognition system into which several tools are integrated to help with the image pre-processing part. By doing so, a machine learning model was developed that does not require a lot of processing power because instead of using the images themselves, it uses extracted data from them to connect this model to a mobile interface that the users will use to recognise signed letters successfully. The communication between the client and the model is sustained through a local server. Introducing sign language into assembly processes is not only a gesture of respect for diversity and inclusion but also a strategic decision that brings tangible benefits. It improves communication, safety, employee morale and overall efficiency, an essential element in achieving operational excellence and an integrated workplace.

Keywords: sign language in assembly process, sign language classifier, machine learning, mobile application

Streszczenie

Język migowy stanowi skuteczny sposób komunikacji dla osób z upośledzeniem słuchu. Proponujemy system rozpoznawania znaków, w którym zintegrowano kilka narzędzi pomagających we wstępnym przetwarzaniu obrazu. W ten sposób opracowano model uczenia maszynowego, który nie wymaga dużej mocy obliczeniowej, ponieważ zamiast korzystać z samych obrazów, wykorzystuje wyodrębnione z nich dane, aby połączyć ten model z interfejsem mobilnym, którego użytkownicy będą używać do skutecznego rozpoznawania podpisanych liter. Komunikacja między klientem a modelem odbywa się za pośrednictwem lokalnego serwera. Wprowadzenie języka migowego do procesów montażowych to nie tylko gest szacunku dla różnorodności i integracji, ale także strategiczna decyzja, która przynosi wymierne korzyści. Poprawia komunikację, bezpieczeństwo, morale pracowników i ogólną wydajność, co jest istotnym elementem w osiąganiu doskonałości operacyjnej i zintegrowanego miejsca pracy.

Słowa kluczowe: język migowy w procesie montażu, klasyfikator języka migowego, uczenie maszynowe, aplikacja mobilna

1. Introduction

Sign language represents an efficient way for individuals with hearing impairments to communicate. A common mistake is to think that the sign language is universal, but it isn't. Deaf people around the world use different sign languages. These gestures, called signs, represent a linguistically structured system of movements and symbols. Three elements make a gestured symbol a sign: the hand's position, shape, and motion. The most used sign language is ASL – short for American Sign Language. (Alliance, 2024).

It's natural to use your hands when speaking to a deaf or hard-of-hearing person. Even if you understand sign language or have a basic grasp of fingerspelling and try to communicate, the impaired person might have trouble understanding you despite your best intentions.

This is an Open Access article distributed under the terms of the Creative Commons Attribution License CC BY 4.0 (https://creativecommons.org/licenses/by/4.0/)

Luckily, technology's ongoing growth and development have created new opportunities for people with hearing loss to bridge the communication barrier. Also, mobile applications have become quite popular in the last few years due to their ability to simplify various aspects of our daily lives. By combining these two, we get the primary motivation behind this paper: provide a user-friendly tool that can easily recognise and interpret sign language to help people both within the deaf community and those who are interested in learning American Sign Language (ASL).

Sign language plays a key role in assembly processes, not only providing a means to overcome communication barriers for deaf and hard-of-hearing people but also helping to improve overall efficiency, safety, and team morale. In an environment where precision and cooperation are essential and where noise often impedes traditional verbal communication, sign language enables the smooth and rapid exchange of information, which is vital to maintaining work continuity and preventing errors.

Safety is a priority in any manufacturing facility, and effective sign language communication allows for immediate warning of potential hazards and response to emergency situations. This significantly reduces the risk of accidents and provides a safer working environment for all employees.

Integrating sign language into the assembly process also has a positive impact on the workplace atmosphere. It promotes a sense of belonging and equality among employees, regardless of their hearing ability. Employees who feel included and valued are more engaged and productive, which translates into better quality work and operational efficiency.

Providing access to training and assembly instructions in sign language is essential to enable deaf and hard of hearing people to participate fully in production processes. This not only makes it easier for them to understand procedures and standards, but also enables them to develop their skills and qualifications, benefiting both employees and the organisation.

Companies that actively integrate sign language into their assembly processes demonstrate greater innovation and flexibility. By embracing diversity and promoting inclusion, they can benefit from the unique perspectives of their employees, often leading to the identification of new solutions and process improvements.

The paper will be structured as follows: The first section, State of the Art, contains a deep analysis of the subject based on theoretical papers and different approaches to solving the problem. The second section, Machine Learning Model, explains the proposed solution from a theoretical point of view, plus the tools and technologies used. The third section, Detailed Design and Implementation, describes the application's development. The Conclusions section contains a paper synthesis and a critical analysis of the results.

2. State of the art

Sign language recognition systems have seen significant advancements in recent years, driven by computer vision, machine learning, and signal processing developments. These systems aim to facilitate communication for individuals with hearing impairments by automatically interpreting sign language gestures.

According to an article by ALTA Language Services, over 300 sign languages are worldwide. About 70 million people worldwide are hearing-impaired and use sign language to communicate.

Like spoken languages, every country has its way of signing, and each might have different dialects (Alta, 2024). Table 1 presents the primary sign languages worldwide (according to Earthweb 2024).

Table 1. Major Sign Languages around the world

Country/ continent	Sign Language	Abbrev.
United Kingdom	British Sign Language	BSL
United States of America	American Sign Language	ASL
Australia	Australian Sign Language	Auslan
Japan	Japanese Sign Language	JSL
People's Republic of China	Chinese Sign Language	CSL
Taiwan	Taiwanese Sign Language	TSL
Middle-East	Arabic Sign Language	ArSL
The Islamic Republic of Iran and other Gulf countries	Persian Sign Language	PSL
India	Indian Sign Language	ISL
Vietnam	Vietnam Sign Language	VSL
Ukraine	Ukrainian Sign Language	UKL
Sri Lanka	Sri Lankan Sign Language	SLTSL
Federative Republic of Brazil	Brazilian Sign Language	Libras
Poland	Polish Sign Language	PJM
The Netherlands	Sign Language of the Netherlands	SLN

(Chai, 2013) Presents how hand gesture recognition influences the sign language recognition system. It focuses on previously used classification methods, compares them, and even suggests the most promising ones for future development.

To fully implement a Sign Language Recognition (SLR) system, feature extraction and recognition methods are needed. When talking about gesture recognition, one of the most complex challenges

encountered is gesture segmentation, meaning knowing when a gesture starts and stops. Fortunately, many methods were developed to pass this challenge. (Suharjitom, 2018).

Recent research has focused on end-to-end deep learning models that directly map sign language videos to text or speech, eliminating the need for intermediate processing steps.

2.1. Machine Learning Model

A machine learning dataset is a compilation of data utilised for model training. It serves as a practical demonstration to instruct the machine learning algorithm on how to make accurate predictions. (Siddharth, 2012) The dataset was divided into training, validation, and test datasets. The training data represents the most critical subset, 60% of the total data. It assists in instructing the algorithm on what specific pattern or elements to identify within the data. After the model is trained, approximately 20% of the overall dataset is allocated for evaluating the model's parameters. The test dataset is used as input in the last stage of the training process and represents the previous 20% of the total data. This dataset has not been used before, so the model is not familiar with it, and it is used to determine the model's accuracy.

Deep learning techniques, particularly convolutional neural networks (CNNs) and recurrent neural networks (RNNs) have shown promising results in sign language recognition. CNNs are effective for extracting spatial features from sign language images, while RNNs are suitable for modelling temporal dependencies in sign sequences.

Google developed MediaPipe Hands, an accurate hand and finger tracking solution. It relies on Machine Learning to detect 21 landmarks. MediaPipe Hands employs a machine-learning pipeline composed of multiple interconnected models: palm detection and hand landmark models (Kaluri, 2017; Manakitsa, 2024).

In Fig. 1, an example of Media Pipe Hands example is presented.

Fig. 1. The 21 critical points of a palm detected by MediaPipe Hands (MediaPipe, online)

During model training, parametrised machine learning is supplied with curated data. This process aims to produce a model with optimised trainable parameters that minimise an objective function. The model's input parameters, also known as hyperparameters, are customisable so that the learning rate of the algorithm behind it will be tuned according to the dataset. Performance metrics, such as accuracy, measure how effectively the model has acquired the desired representation. They provide insights into the model's performance, indicating how well it has learned from the data. Enhanced model performance translates into various real-life advantages, such as increased revenue, lowered costs, or improved user experience. Model validation is required because every algorithm presents different performances based on datasets. If the accuracy score of the model is low, the hyperparameters can be changed until the desired accuracy level is reached. In other words, validating machine learning model outputs is essential to guarantee accuracy. A substantial amount of training data is employed during the training of a machine learning model. The primary purpose of conducting model validation is to enhance the quality and quantity of data by identifying areas for improvement.

3. Detailed Design and Implementation

3.1. Application architecture

The Client-Server architecture of the American sign language recognition application is presented in Fig. 2.

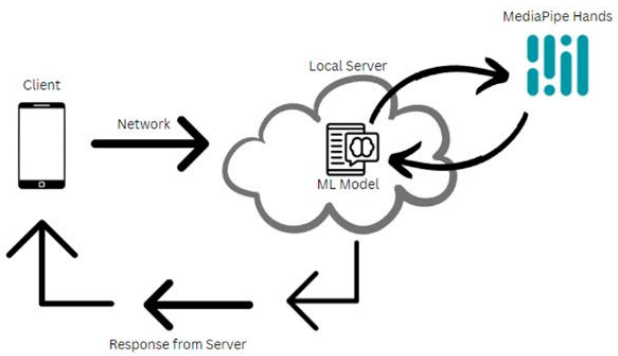

Fig. 2. Client–Server Architecture of the application

The client application is represented by the mobile application developed. The app user can upload an image or capture it using the device's camera, thus initiating a request to send the image to the server. The request is for type HTTP, specifically POST.

The server, running on localhost, listens for incoming requests and handles them by receiving the images sent by the client. The image is then sent to MediaPipe Hands API, which processes it and extracts the coordinates of the 21 critical points of a hand.

MediaPipe also draws on those coordinates' images to better visualise how the hand was perceived.

Next, the set of 3D coordinates, along with the image containing the landmarks, are sent back to the server where the trained machine learning model that can classify letters of the American sign language is hosted. Based on the coordinates received as input, the model categorises the letter.

Finally, the detected letter and the image with landmarks are sent back to the client as a response from the server. The user will see the reaction on the screen. This whole process can be repeated multiple times.

An important aspect to consider is the privacy of the application's users. Storing user-generated images can pose privacy and security risks, mainly if a virus attacks the server. Images may contain sensitive and personal information, and the user does not consent to storing or sharing their pictures. By not saving the photos, the risk of data breaches is minimised.

3.2. Sign language recognition model

The dataset can determine whether the model is good or not. The model's performance improves as the dataset size increases. An existing dataset from Keggle was chosen. It already contains about 87.000 images of the alphabet letters from the American sign language. In addition to this dataset, several hundred pictures collected in the laboratory environment were used.

The dataset was divided into two sets, with an 80% to 20% ratio. 80% of the data was used to train the model, while 20% was used to validate it.

When training the model, it was observed that MediaPipe Hands did not find all the images to contain hands. That's because although the dataset is numerous, the images are 200x200 pixels. Because of the poor quality of the photos, MediaPipe could not identify a hand in most of the pictures. To solve this issue and to avoid going through the entire dataset manually, a script was used to send the images to MediaPipe before the actual training. If a hand was detected, the respective image was saved in the "training_dataset" folder and labelled accordingly in the format 'letter' + 'image_number'. After this entire process, the training dataset consisted of only 25.000 images.

3.3. Model Training and Validation

Model training is the most crucial phase of developing a sign language recognition system employing machine learning techniques.

The model is formed from 6 layers: 1 input layer, two dropout layers, and three dense layers.

The training process involves using the fit function, where both the number of epochs and the validation data are specified, and the callbacks are used to perform specific tasks at specific stages during the training process. The total number of epochs is 10000, and the batch size is 4096 units. After the training phase, the model's performance can be evaluated based on the measured accuracy. From the logs received at the end of the training, we see that the model has an impressive accuracy score of 0.9019 and a loss score of 0.3267. In percentage, this means that the model's overall accuracy is 90%. In addition, the confusion matrix, see Fig. 3, was generated to conduct a more detailed analysis of the model's performance.

It was tested with new data using the mobile application to validate that the model was behaving as expected. In Fig. 4, two images are attached: the first represents the proof of the actual letter, while the second represents the model's response to the same image.

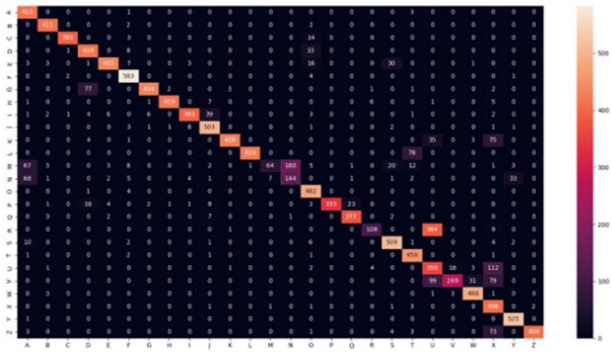

Fig. 3. Confusion matrix of the NN model

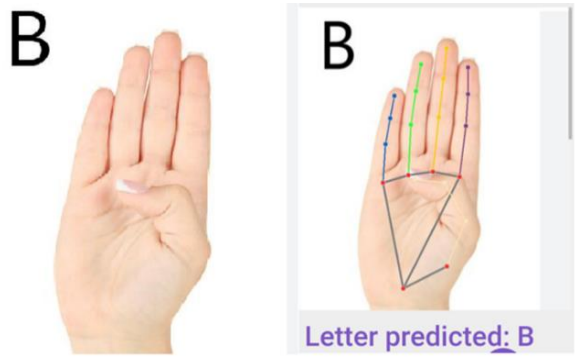

Fig. 4. Reference image vs Model prediction for B letter

After entering the application, the user is directed to the first page of the app, presented in Fig. 5. This page acts as the main page and has the functionality of a dashboard. A list of signs is displayed as the main content of the screen. Each sign is labelled with the scope of helping the user accommodate the letters and how they should be signed.

Fig. 5. The main screen of SignSense

Postman was used to test and validate that the server's services function accordingly. The testing method mainly focused on communication between the server and the client. In other words, the response to every request was tested.

We expect that every call responds with a 200-status code and that the server successfully receives the image sent as input from the request's header. The server's response can be observed even in the terminal in the form of logs.

During the implementation phase, client testing was done with an emulator provided by Android Studio. This helped mimic real-world scenarios without the need for an actual physical device. Also, because Flutter offers a hot reload functionality, it was beneficial from a time perspective because any change could be seen more easily on the emulator.

4. Conclusions

This paper has focused on developing a functional mobile application to recognise and classify American Sign Language (ASL) letters. By implementing the machine learning models based on CNN for signs classification, the accuracy was above 90%. The ML model training needs thousands of iterations for each sign. The application implemented in this paper makes a valuable contribution to advancing technology-based solutions to enhance communication and accessibility by harnessing the power of machine learning and mobile technology. It highlights that, through ongoing research and development in these fields, we can aspire for a future where technology-based solutions are easily accessible, user-friendly, and integrated into our everyday lives, enriching the experiences of all individuals.

Sign language in production processes is not only a communication tool, but also an important element building a safe, integrated and innovative workplace. The promotion and implementation of this language reflects the desire to create open, accessible and friendly development of technologies supporting sign language opens new possibilities for the integration and efficiency of production processes. Thanks to tools such as real-time translation applications or videoconferencing with interpreters, deaf and hard of hearing people can fully use their skills and competences, contributing to the success of the company.

This study highlights how technology-driven solutions can improve accessibility and communication for members of the deaf and hard-of-hearing community. Moreover, it represents a tool anyone can use to learn the basics of the American sign language: the alphabet. However, there is still room for improvement so that the application could fully satisfy the needs of the deaf community and their acquaintances.

The first improvement that comes to mind is extending the application's capabilities to perform real-time recognition of the American Sign Language from live video streams.

References

Adithya V. and Rajesh R.. 2020. *A deep convolutional neural network approach for static hand gesture recognition.* Procedia Comput. Sci. 171 (2020), 2353–2361.

ALTA (2024). *Deaf culture and sign language.* https://www.altalang.com/beyond-words/deaf-culture-and-sign-language/

Assael, Y. M., Shillingford, B., Whiteson, S., & de Freitas, N. (2016). *LipNet: Sentence-level Lipreading.* Computing Research Repository (CoRR), 1611.01599, 1-13.

http://arxiv.org/abs/1611.01599

Bhavsar, H. (2017). *Review of Classification Methods Used in Image-based Sign Language Recognition System.* International Journal on Recent and Innovation Trends in Computing and Communication, 5(5), 949–959.

Bhavsar, H., & Trivedi, J. (2017). *Review of feature extraction methods for image-based sign language recognition systems.* Indian Journal of Computer Science and Engineering (IJCSE), 8(3), 249-259.

Cao, Y., Chou, P. A., Zhang, Z., & Park, H. S. (2018*). Recent advancements in deep learning for sign language recognition: A review.* Computer Vision and Image Understanding, 171, 130-140.

Chai, X., Li, G., Lin, Y., Xu, Z., Tang, Y., Chen, X., & Zhou, M. (2013). *Sign language recognition and translation with Kinect.* In Proceedings of IEEE International Conference on Automatic Face and Gesture Recognition (pp. 1-2). Shanghai, China.

Costa Filho, C. F. F., Souza, R. S. de, Santos, J. R. dos, Santos, B. L. dos, & Costa, M. G. F. (2017). *A fully automatic method for recognising hand configurations of Brazilian sign language.* Research on Biomedical Engineering, 33(1), 78–89.

Earthweb (2024). *Sign language users.* https://earthweb.com/sign-language-users/.

Elmezain, M., Al-Hamadi, A., Appenrodt, J., & Michaelis, B. (2008). *A hidden Markov model-based continuous gesture recognition system for hand motion trajectory.* In Pattern Recognition, 2008. ICPR 2008. 19th International Conference on (pp. 1–4). Tampa, FL, USA.

Escobedo, E., & Camara, G. (2016). *A new Approach for Dynamic Gesture Recognition using Skeleton Trajectory Representation and Histograms of Cumulative Magnitudes.* In SIBGRAPI Conference on Graphics, Patterns, and Images (pp. 209–216). São Paulo, Brazil.

Ghosh, D. K., & Ari, S. (2016). *On an algorithm for Vision-based hand gesture recognition*. Signal, Image and Video Processing, 10(4), 655–662.

Jayanthi Palraj, R K Ponsy, K Swetha, S A Subash. (2022). *Real-Time Static and Dynamic Sign Language Recognition using Deep Learning.* Journal of Scientific & Industrial Research 81(11):1186-1194. DOI: 10.56042/jsir.v81i11. 52657.

Kakde, M. U., Nakrani, M. G., & Rawate, A. M. (2016). *A Review Paper on Sign Language Recognition System For Deaf And Dumb People using Image Processing. International.* Journal of Engineering Research and Technology, 5(3), 590–592.

Kalsh, E. A., & Garewal, N. S. (2013). *Sign Language Recognition System*. International Journal of Computational Engineering Research, 3(6), 15-21.

Kaluri, R., & Pradeep, C. H. (2017). *An enhanced framework for sign gesture recognition using hidden Markov model and adaptive histogram technique.* International Journal of Intelligent Engineering & Systems,10(3), 11-19.

Manakitsa N, Maraslidis GS, Moysis L, Fragulis GF. (2024). *A Review of Machine Learning and Deep Learning for Object Detection, Semantic Segmentation, and Human Action Recognition in Machine and Robotic Vision.* Technologies.12(2):15. https://doi.org/10.3390/technologies12020015.

MediaPipe, "MediaPipe Documenation", [Online]. Available: https://developers.google.com/mediapipe/solutions/vision/hand_landmarker.

Naik BT, Hashmi MF, Bokde ND. (2022). A Comprehensive Review of Computer Vision in Sports: Open Issues, Future Trends and Research Directions. Applied Sciences. 2022; 12(9):4429. https://doi.org/10.3390/app12094429.

Nimratveer Kaur Bahia, Rajneesh Rani. (2023). *Multi-level Taxonomy Review for Sign Language Recognition: Emphasis on Indian Sign Language.* ACM Transactions on Asian and Low-Resource Language Information Pro-cessingVolume 22Issue 1Article No.: 23pp 1–39https://doi.org/10.1145/3530259.

Siddharth Rautaray, Anupam Agrawal, (2012). *A comprehensive review of vision-based hand gesture recognition.* Artificial Intelligence Review 43(1). DOI: 10.1007/s10462-012-9356-9.

Suharjitom F. W. G. P. K., Meita Chandra Ariesta. (2018). *A Survey of Hand Gesture Recognition Methods in Sign*. Pertanika Journal of Science and Technology, p. 19, 2018.

The Alliance for Access to Computing Careers (2024). *Deaf or Hard of Hearing.* https://www.washington.edu/accesscomputing/what-sign-language.

Technologia i Automatyzacja Montażu

Volume 123, Issue 1/2024, Pages 16-22
https://doi.org/10.7862/tiam.2024.1.3

Original Research

OPTIMIZING THE SIMULATION OF CONVEYOR SYSTEMS THROUGH DIGITAL SHADOW INTEGRATION TO INCREASE ASSEMBLY PROCESS EFFICIENCY

OPTYMALIZACJA SYMULACJI SYSTEMÓW PRZENOŚNIKÓW POPRZEZ INTEGRACJĘ CYFROWEGO CIENIA DLA ZWIĘKSZENIA WYDAJNOŚCI PROCESU MONTAŻU

Jozef HUSÁR[1,*], Stella HREHOVA[1], Piotr TROJANOWSKI[2], Markus BRILLINGER[3]

[1] Department of Industrial Engineering and Informatics, Technical University of Košice, Faculty of Manufacturing Technologies with a seat in Prešov, Bayerova 1, 080 01 Prešov, Slovak Republic
[2] Department of Logistics and Transport Economics, Faculty of Maritime Technology and Transport, West Pomeranian University of Technology in Szczecin, 17, Piastów Ave., 70-310, Szczecin, Poland
[3] Pro2Future GmbH, Inffeldgasse 25f, 8010 Graz, Austria

* Corresponding author: jozef.husar@tuke.sk tel.: (+421 55 602 6415)

Abstract

In today's highly competitive industrial environment, continuous improvement of efficiency and optimization of processes is crucial. This paper presents an approach to the optimization of conveyor systems that uses the concept of a digital shadow. A digital shadow, as an exact digital replica of a physical conveyor system, enables detailed simulation and analysis of real operational data, providing a basis for in-depth analysis and identification of areas for improvement. The aim of this approach is not only to improve the understanding of the dynamics and performance of existing conveyor systems, but also to increase the overall efficiency through predictive simulations and optimization algorithms. In this work, we demonstrate how the integration of a digital shadow into the simulation process can contribute to a better reaction to changes in the production environment, to the reduction of downtime and to the optimization of production flows. Our methodology combines data collection / analysis, and enables the creation of accurate and flexible models of conveyor systems. These models are then used in simulations that help identify optimal settings for different production scenarios and predict potential problems before they occur. The results of applying our approach on a test laboratory line show a significant improvement in efficiency and a reduction in operating costs. This study provides important insights and practical guidelines for engineers and production managers focused on the use of digital shadow to increase the efficiency of conveyor systems. It also contributes to the development of intelligent production technologies in the era of Industry 4.0.

Keywords: conveyor system, simulation, digital shadow, efficiency

Streszczenie

W dzisiejszym wysoce konkurencyjnym środowisku przemysłowym kluczowe znaczenie ma ciągła poprawa wydajności i optymalizacja procesów. W artykule przedstawiono podejście do optymalizacji systemów przenośnikowych wykorzystujące koncepcję cyfrowego cienia. Cyfrowy cień, jako dokładna cyfrowa replika fizycznego systemu przenośników, umożliwia szczegółową symulację i analizę rzeczywistych danych eksploatacyjnych, dając podstawę do dogłębnej analizy i identyfikacji obszarów wymagających poprawy. Celem tego podejścia jest nie tylko lepsze zrozumienie dynamiki i wydajności istniejących systemów przenośników, ale także zwiększenie ogólnej wydajności poprzez symulacje predykcyjne i algorytmy optymalizacyjne. W tej pracy pokazujemy, jak włączenie cienia cyfrowego do procesu symulacji może przyczynić się do lepszej reakcji na zmiany w środowisku produkcyjnym, ograniczenia przestojów i optymalizacji przepływów produkcyjnych. Nasza metodologia łączy zbieranie/analizę danych oraz umożliwia tworzenie dokładnych i elastycznych modeli systemów

This is an Open Access article distributed under the terms of the Creative Commons Attribution License CC BY 4.0 (https://creativecommons.org/licenses/by/4.0/)

przenośnikowych. Modele te są następnie wykorzystywane w symulacjach, które pomagają zidentyfikować optymalne ustawienia dla różnych scenariuszy produkcji i przewidzieć potencjalne problemy, zanim one wystąpią. Wyniki zastosowania naszego podejścia na linii laboratorium badawczego wskazują na znaczną poprawę wydajności i redukcję kosztów operacyjnych. Niniejsze badanie dostarcza ważnych spostrzeżeń i praktycznych wskazówek dla inżynierów i kierowników produkcji skupiających się na wykorzystaniu cyfrowego cienia w celu zwiększenia wydajności systemów przenośników. Przyczynia się także do rozwoju inteligentnych technologii produkcyjnych w dobie Przemysłu 4.0.

Słowa kluczowe: system przenośników, symulacja, cień cyfrowy, wydajność

1. Introduction

In today's rapidly changing industrial environment, there is a constant need to increase efficiency and optimize production processes. One of the cornerstones of modern production systems is conveyor systems, which play a key role in automating and streamlining assembly lines. Thanks to their ability to efficiently move materials and components among different parts of the manufacturing process, conveyor systems are an integral part of industrial production. However, in order to achieve maximum efficiency and minimize outages, it is necessary to constantly monitor and optimize their performance Antosz et al. (2019).

Traditional methods of monitoring and optimization often rely on manual intervention and post-hoc analysis, which cannot adequately address the dynamic nature of production processes. In this context, the integration of the digital shadow, a concept based on the field of Industry 4.0, offers a revolutionary approach to the optimization of conveyor systems Kluz et al. (2019). The digital shadow, as a virtual replica of the physical system, records and analyzes data in real time, providing a comprehensive overview of the current state and performance of the conveyor system.

The use of digital shadowing in the context of simulation and optimization of conveyor systems enables accurate bottlenecks identification, prediction of potential problems and material flow optimization Husar et al. (2019) . This methodology makes it possible to create simulations that can predict system performance under different operating conditions and settings, leading to significant improvements in assembly efficiency and reductions in downtime and maintenance costs. At the same time, integrating a digital shadow into the optimization process allows changes to be made and their impact simulated in a safe, virtual environment, eliminating the need for costly and time-consuming real-world tests. This approach not only increases the adaptability and flexibility of production systems, but also enables faster implementation of innovations and improvements Malopolski et al. (2018).

In addition, the use of advanced analytics tools and machine learning algorithms within the digital shadow enables continuous optimization and learning from historical data, increasing the accuracy of predictions and the efficiency of decision-making processes. This approach supports the development of intelligent, self-regulating systems that can dynamically respond to changes in the operating environment and maintain a high level of performance without the need for external intervention. In this paper, we present a comprehensive overview of how digital shadow integration can radically change the approach to simulation and optimization of conveyor systems Van Vianen et al. (2016). We explore various strategies and technologies that enable effective use of digital shadowing to improve assembly processes, and discuss potential challenges and solutions in implementing these technologies in practice. The aim is to provide readers with an in-depth look at the benefits and possibilities that the digital shadow brings to industrial manufacturing and highlight its key role in the transformation towards more efficient and intelligent manufacturing systems Trojanowska et al. (2023).

1.1. Simulation of conveyor systems

Subsequently, we will focus on the importance and meaning of the conveyor systems simulation in the context of digital shadow integration, as a tool for improving efficiency and optimizing processes in industrial assembly. The simulation of conveyor systems is a critical step in the process of planning and optimizing production lines. Using digital modeling and simulation, various aspects of conveyor systems can be virtually tested and analyzed, including their configuration, capacity, speed and interaction with other components of the production process Kawa et al. (2016). This approach allows engineers and designers to identify potential problems and bottlenecks in the process before the system is physically implemented, greatly reducing modification costs and increasing the overall efficiency of assembly operations Graczyk-Tarasiuk et al. (2022).

Integrating a digital shadow into the simulation process brings another level of accuracy and detail to the analysis. Collecting real-time data from physical

systems, the digital shadow provides up-to-date and accurate information on the health and performance of existing conveyor systems. This information is subsequently used in the simulation, which increases the relevance and applicability of the obtained results to real production situations Lazar et al. (2012). This synergy between digital shadowing and simulation makes it possible to create highly accurate models that can predict the results of changing configuration, workload or operational parameters with unprecedented accuracy.

In practice, the conveyor systems simulation enables a comprehensive assessment of various aspects of production processes. For example, it can help decide the optimal speed of movement on conveyor belts to maximize production capacity while minimizing equipment wear and energy consumed to operate it. Simulations can also reveal inefficient layouts of production lines, allowing them to be reconfigured for smoother material flow and reduced time lost in transportation among individual production sites Kolny et al. (2023).

Another key aspect is the ability to simulate conveyor systems to support predictive maintenance. Analysis of data from the digital shadow makes it possible to identify patterns that prevent component failures and wear. In this way, maintenance work and part replacements can be planned before they could cause serious production interruptions or expensive repairs.

Together, simulation and the digital shadow provide the basis for creating adaptive and intelligent manufacturing systems. These systems are able to dynamically respond to changes in demand, material flows and operating conditions, thereby increasing their efficiency and flexibility. The practical implementation of these technologies means for industrial enterprises not only an improvement in performance, but also an increase in competitiveness on a global scale. However, despite these advantages, the integration of digital shadow and simulation of conveyor systems presents some challenges. These include ensuring data quality and integrity, processing huge data volumes in real-time, and creating accurate models that adequately reflect reality. In addition, there is a need to overcome cultural and organizational barriers that may hinder the adoption and effective implementation of these advanced technologies Kawa et al. (2016). The conveyor systems simulation with digital shadow integration opens up new possibilities for optimizing and streamlining industrial assembly lines. It offers in-depth insight into operational performance, enables predictive maintenance and supports fast and informed decision-making. With appropriate investments in technology and a change in mindset, this integration can significantly contribute to achieving higher levels of industrial efficiency and adaptability in an ever-changing global economic environment.

1.2. Literature review

Optimizing the simulation of conveyor systems through digital shadow integration can increase assembly efficiency. By creating digital twins or digital shadows of production systems, companies can limit physical test runs and reduce costs Kassen et al. (2021). These digital twins can mirror the current stage of the physical pallet transportation process and predict transportation times, allowing for optimized product scheduling and resource allocation Raileanu et al. (2019). Implementing range-inspection control (RIC) in automated conveyor systems can further optimize their operation within the smart manufacturing framework Wang et al. (2022). Model-based design and simulation can be used to achieve optimal efficiency of conveyor belts, improving productivity in advanced manufacturing environments Salawu et al. (2020). Virtual commissioning and simulation tools like Siemens Tecnomatix Process Simulate can be used to design and test control systems for conveyors, increasing efficiency and reducing the risk of damage to functional parts Ruzarovsky et al. (2018).

Simulation of conveyor systems through digital shadow is a valuable tool in the design and optimization of conveyor control systems. By creating a virtual model of a real conveyor, engineers can test and evaluate different scenarios without the need for physical intervention or potential damage to functional parts Mikušova et al. (2019). This approach allows for the integration and testing of control systems through simulation before the physical construction of the conveyor, saving time and resources Li et al (2011). The use of simulation language and regression models further enhances the ability to test proposed changes and improve the functionality of the conveyor in real-world operations Pathak et al. (2021). The combination of digital technology and traditional shadow puppets has also been explored, allowing users to manipulate and control digital shadow props in a user-oriented and interactive manner Tri handoyo at el. (2010). Overall, simulation and digital shadow techniques offer significant benefits in the design, optimization, and performance of conveyor systems.

2. Methodology

The digital shadow creation of the conveyor system is based on the concept of the SmartTechLab laboratory for Industry 4.0 shown in Figure 1. The selected laboratory is located at the Faculty of Manufacturing Technologies, located in Prešov,

Technical University of Košice. This laboratory is focused on industry 4.0 and smart technologies Kovbasiuk et al. (2023).

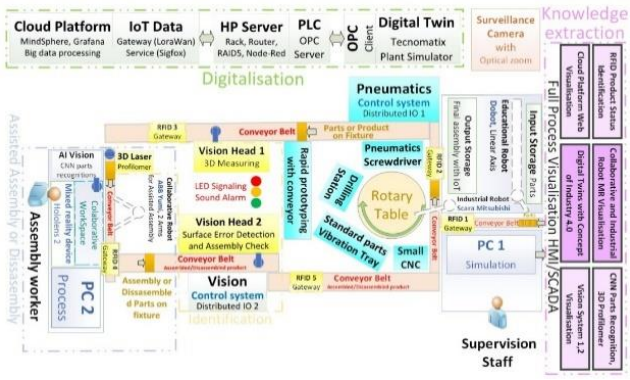

Fig. 1. SmartTechLab concept for industry 4.0

As can be seen from the picture, the system arrangement principle consists of 4 conveyors arranged in a closed cycle. There are 6 conveyors, 3 conveyors with a width of 20 cm and 3 conveyors with a width of 8 cm. Control of the electric motors is provided by frequency converters for speed control connected to a central PLC that performs complex logic operations and controls various aspects of the conveyor operation, such as speed, direction and coordination between multiple conveyor segments. In the presented article, we created a layout model in the 2D interface of the simulation tool Tecnomatix Plant Simulation Židek et al. (2021).

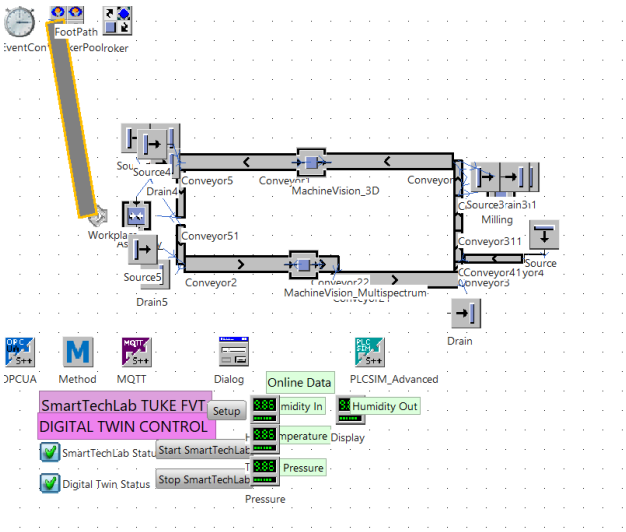

Fig. 2. 2D model of conveyor system

Tecnomatix Plant Simulation provides robust conveyor system modeling benefits that are key to optimizing and analyzing manufacturing processes. With its advanced simulation capabilities, it enables users to efficiently model and simulate complex conveyor systems, reducing the need for physical prototypes and shortening the time needed for experimentation. Tecnomatix Plant Simulation supports a detailed analysis of material and information flow, enables accurate prediction of the various scenario impacts on the overall efficiency of the production system. This ability to predict and optimize the performance of the conveyor system before its physical implementation significantly reduces production costs and increases productivity. In addition, the flexible and user-friendly Tecnomatix Plant Simulation platform supports rapid adaptation to changes in projects, thereby improving the ability to respond to dynamic market demands and increasing the competitiveness of manufacturing companies.

Based on the disposition model of Fig.3, a digital shadow was subsequently created.

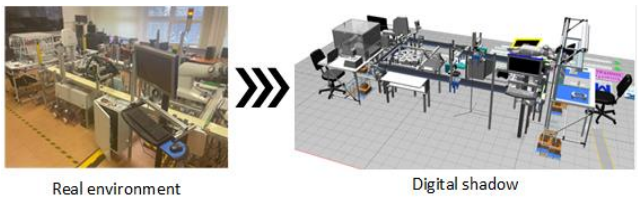

Fig. 3. SmartTechLab concept for industry 4.0

In the digital shadow, users can customize a wide range of conveyor settings, including conveyor speed, capacity, type (belt, roller, chain), movement direction, accumulation method, start and stop conditions, as well as interaction with other objects and response to disturbances.

These settings are crucial for accurate modeling and simulation of conveyor systems, enabling efficient layout planning, optimization of material and information flow, as well as realistic simulation of work cycles and responses to unexpected events. This detailed level of customization supports in-depth analysis and production process improvement.

Fig. 4. Setting the conveyor's basic parameters

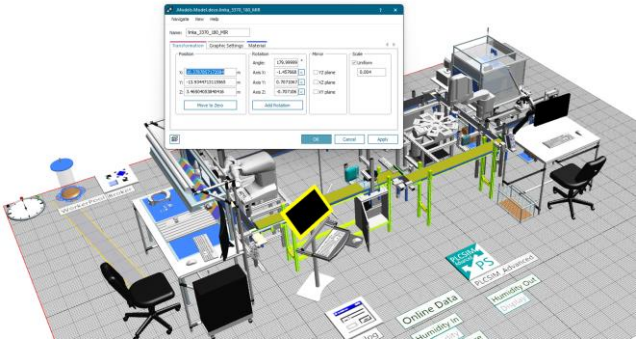

Fig. 5. Setting the conveyor's dimensional parameters

The presented digital shadow is a universal tool for simulating the selected transport system. In addition to conveyor parameters, it is also possible to edit objects moving along the conveyor. As already mentioned, the conveyor systems are 20 cm and 8 cm wide, therefore, for our needs, a preparation of a handling pallet with dimensions of 18 x 7.5 cm was created. The universal handling pallet is an innovative solution, designed to adapt to different sizes and shapes of loads, thereby increasing the efficiency of handling materials and optimizing the use of warehouse space. This flexibility is crucial in dynamic manufacturing and distribution environments where the requirements for transporting and storing materials are constantly changing. The universal handling pallet enables quick and efficient configuration changes as needed, which reduces the time required for load preparation and minimizes the need for different specific pallets for different types of products.

Thanks to its modularity and adaptability, the universal handling pallet can support a wide range of loads – from small components to large and heavy objects – ensuring stable and safe storage and transport.

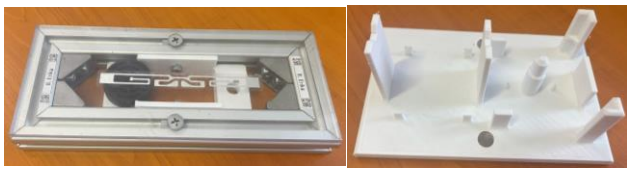

Fig. 6. Universal palette and preparation for handling

This type of pallet often includes adjustable or replaceable components, such as sidewalls, space dividers or customizable mounts, which ensure that it can effectively serve a wide range of applications regardless of the load specifics. Such versatility and adaptability make the universal handling pallet a valuable tool for lines looking for ways to improve their logistics operations while reducing costs and environmental impact by minimizing the need for multiple types of packaging materials.

3. Results

In the article, we present a digital model of a conveyor line on which all parameters can be modified according to real data obtained by observation and measurement. In our model, we included several operations with a specific time and we gradually added to the empty pallet in the model the preparation, plastic components that were put together in the assembly workplace to form the final product representing the cam switch.

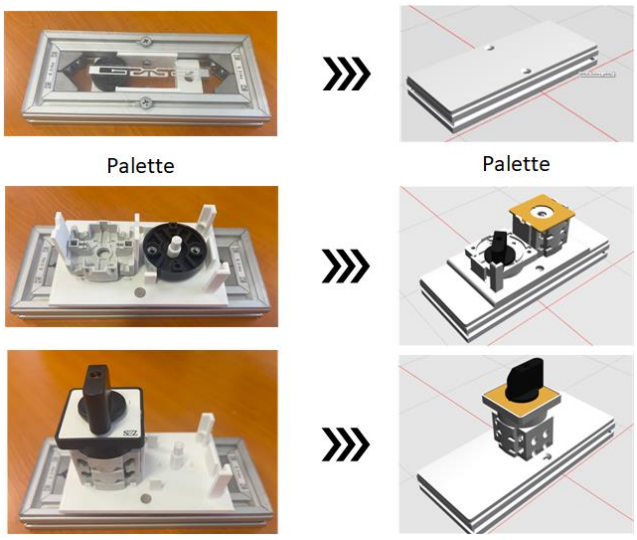

Fig. 7. A view at real components and elements for simulation / digital shadow

In order to increase efficiency, we gradually began to optimize the cam switch assembly process. As part of the simulation, we gradually changed the amount of products in the production batch in the range of 10 pcs to 100 pcs available in 10 pcs increments. In doing so, we analyzed the ratio of performed operations to transport and storage. From the obtained results, it is obvious that the processes did not change, but with a larger number of pieces, the ratio of total transportation began to decrease from 70% to 60%, which represents a saving of 10% of the total time. In the model proposed by us, downtime and blocking times of individual operations have been eliminated. In our case study, in the next steps we optimized the speed of the conveyors in the simulation model, we implemented the optimization of the times of the components placed on the stage, and we also tried to optimize the individual operations activities using robotic workplaces.

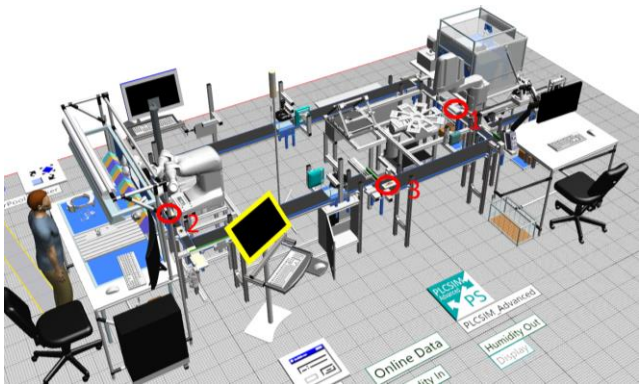

Fig. 8. Simulation model/digital shadow of a conveyor system with pallets

We can see 3 positions on the presented model. The first position represents the empty pallet arrival on which plastic components are gradually placed on a rotary table using the SCARA robot. The second position represents an assembly workplace with assisted assembly using the collaborative robot ABB Yuma and a human, and the third position represents the movement of a folded cam switch after exit inspection using a camera system directed to the exit warehouse. The movement of pallets is solved using the conveyor system described in chapter 2. The digital shadow represents an advanced digital replica of physical systems, allowing detailed monitoring, analysis and prediction of their performance based on real-time data collection and processing. In the context of our research, the digital shadow serves as the basis for the simulation and the conveyor system optimization used in the cam switch assembly process. Thanks to the integration of the digital shadow, we are able to virtually model the entire production process, adjust the simulation parameters according to real data and effectively optimize operations, thereby increasing the overall efficiency of assembly.

Our simulated model, including a digital shadow, allows detailed observation and modification of all relevant parameters. This approach not only increases the simulation accuracy but also provides valuable insight into possible optimizations. The optimization of the simulated model based on the digital shadow brought a significant improvement in the efficiency of the assembly process. Additionally, our case studies have shown that by optimizing conveyor speeds and component timing, we can further increase efficiency, while the integration of robotic workplaces into individual operations enables greater accuracy and assembly speed. The results of our study clearly show that the digital shadow represents a powerful tool for the simulation and production process optimization. Its ability to accurately reflect and predict the performance of physical systems opens up new possibilities for more efficient and flexible manufacturing operations. With this approach, it is possible not only to increase the efficiency of existing processes, but also to adapt to rapidly changing production requirements and ensure a competitive advantage in a dynamic industrial environment.

4. Conclusion

In a dynamic and constantly evolving industrial environment, the need to increase the efficiency of production processes becomes a focus for many organizations. Optimizing the conveyor systems simulation through digital shadow integration opens up new horizons for improving assembly efficiency. This approach, consisting of the connection of the virtual and physical world, brings significant benefits in the form of more accurate modeling, analysis and prediction of the conveyor systems performance. In the course of this article, we have explored how the integration of the digital shadow into simulations enables businesses to gain better understanding and control over their handling processes. Demonstrating a case study and theoretical concepts, we highlighted that the digital shadow offers a unique opportunity not only for monitoring and analyzing the current state of conveyor systems, but also for predicting future performance and possible problems. The key to success is the digital shadow's ability to acquire, analyze and apply real-time data, enabling a quick and efficient response to any changes or necessary adjustments.

This adaptive approach significantly reduces downtime, improves productivity and minimizes waste in assembly processes. In addition, the use of advanced machine learning algorithms and artificial intelligence within the digital shadow can further increase the accuracy of simulations and predictions, opening up new possibilities for optimizing production processes. In conclusion, the integration of digital shadow into the conveyor systems simulation represents a significant step forward in the field of industrial efficiency. It not only offers the opportunity to improve current operations but also provides a platform for innovation and improvement of future production processes. As we have shown, this approach has the potential to transform the way businesses approach the optimization of their production lines and has a significant impact on increasing assembly efficiency. Armed with this knowledge, businesses are better prepared to face the challenges of Industry 4.0 and take advantage of the opportunities that digitization brings.

Acknowledgments

This work was supported by the projects VEGA 1/0268/22, KEGA 038TUKE-4/2022 granted by the

Ministry of Education, Science, Research and Sport of the Slovak Republic.

References

Antosz K., Pasko L., Gola A, (2019) The Use of Intelligent Systems to Support the Decision-Making Process in Lean Maintenance Management, IFAC PapersOnLine 52-10, pp. 148-153. https://doi.org/10.1016/j.ifacol.2019.10.005

Graczyk-Tarasiuk, J., Karyono, K., & Karyono, K. (2022). The framework for the supplier qualification system for the world leader home appliances industry. Technologia I Automatyzacja Montażu (Assembly Techniques and Technologies), 116(2), 41-52. https://doi.org/10.7862/tiam.2022.2.6

Husar, J., Knapcikova, L., Balog, M. (2019). Implementation of Material Flow Simulation as a Learning Tool. In: Ivanov, V., et al. Advances in Design, Simulation and Manufacturing. DSMIE 2019. Lecture Notes in Mechanical Engineering. Springer, Cham. https://doi.org/10.1007/978-3-319-93587-4_4

Kassen, S., Tammen, H., Zarte, M., Pechmann, A. (2021) Concept and Case Study for a Generic Simulation as a Digital Shadow to Be Used for Production Optimisation. Processes, 9, 1362. https://doi.org/10.3390/pr9081362

Kawa, A., Fuks, K., Januszewski, P. (2016). Computer Simulation as a Research Method in Management Sciences, Studia Oeconomica Posnaniensia, no. 1, t. 4: 109-127.

Kluz, R., Antosz, K. (2019). Simulation of Fliexible Manufacturing Systems as an Element of Education Towards Industry 4,0. In: 6th International Scientific Technical Conference on Advances in Manufacturing II (Manufacturing): 332-341. https://doi.org/10.1007/978-3-030-18715-6_28.

Kolny, D., Kaczmar-Kolny, E., & Dulina, Ľuboslav. (2023). Modeling and simulation of the furniture manufacturing and assembly process in the arena simulation software . Technologia i Automatyzacja Montażu (Assembly Techniques and Technologies), 119(1), 13-22. https://doi.org/10.7862/tiam.2023.1.2

Kovbasiuk, K., Demčák, J., Husár, J., Hošovsky, A., Hladký, V. (2023). A Digital Twin for Remote Learning: A Case Study. In: Ivanov, V., Trojanowska, J., Pavlenko, I., Rauch, E., Piteľ, J. (eds) Advances in Design, Simulation and Manufacturing VI. DSMIE 2023. Lecture Notes in Mechanical Engineering. Springer, Cham. https://doi.org/10.1007/978-3-031-32767-4_36

Lazar, I., Husar, J. (2012). Validation of the serviceability of the manufacturing system using simulation. J. Effi. Responsib. Educ. Sci. 5(4), 252–261. https://doi.org/10.7160/eriesj.2012.050407

Li, Q., Hua, Qy., Feng, J., Niu, W., Wang, H., Zhong, J. (2011). Design and Implementation of Interactive Digital Shadow Simulation System. In: Ma, M. (eds) Communication Systems and Information Technology. Lecture Notes in Electrical Engineering, vol 100. Springer, Berlin, Heidelberg. https://doi.org/10.1007/978-3-642-21762-3_24

Malopolski, W., Wiercioch, A. (2018). An Approach to Modeling and Simulation of a Complex Conveyor System Using Delmia Quest–A Case Study. In: Hamrol, A., Ciszak, O., Legutko, S., Jurczyk, M. (eds) Advances in Manufacturing. Lecture Notes in Mechanical Engineering. Springer, Cham. https://doi.org/10.1007/978-3-319-68619-6_58

Mikušová, N., Stopka, O., Stopková, M. & Opettová, E. (2019). Use of simulation by modelling of conveyor belt contact forces. Open Engineering, 9(1), 709-715. https://doi.org/10.1515/eng-2019-0070

Pathak, S. D., Luitel, A., Singh, S. & Pandey, R. (2021) Second Generation Voltage Conveyor II based Shadow Filter, 2021 2nd International Conference for Emerging Technology (INCET), Belagavi, India, 2021, pp. 1-5, https://doi.org/10.1109/INCET51464.2021.9456370.

Răileanu, S., Borangiu, T., Ivănescu, N., Morariu, O. & Anton, F. (2020). Integrating the Digital Twin of a Shop Floor Conveyor in the Manufacturing Control System. In: Borangiu, T., Trentesaux, D., Leitão, P., Giret Boggino, A., Botti, V. (eds) Service Oriented, Holonic and Multi-agent Manufacturing Systems for Industry of the Future. SOHOMA 2019. Studies in Computational Intelligence, vol 853. Springer, Cham. https://doi.org/10.1007/978-3-030-27477-1_10

Ruzarovsky, R., Holubek, R., Delgado Sobrino, D. R., & Janíček, M. (2018). The Simulation of Conveyor Control System Using the Virtual Commissioning and Virtual Reality. Advances in Science and Technology Research Journal, 12(4), 164-171. https://doi.org/10.12913/22998624/100349

Salawu, G., Bright, G. & Onunka, Ch. (2020). Modelling and simulation of a conveyor belt system for optimal productivity, International Journal of Mechanical Engineering and Technology (IJMET), 11(1), pp. 115-121. https://doi.org/10.34218/IJMET.11.1.2020.012

Tri handoyo, I., Subali, M. (2010). Conveyor control system based on high low at89s51 microcontroller-based products. pp.1-14.

Trojanowska, J., Husár, J., Hrehova, S. & Knapčíková, L. (2023) Poka Yoke in Smart Production Systems with Pick-to-Light Implementation to Increase Efficiency. Appl. Sci. 2023, 13, 11715. https://doi.org/10.3390/app132111715

Van Vianen, T., Ottjes, J. & Lodewijks, G. (2016) Belt conveyor network design using simulation. J Simulation 10, 157–165. https://doi.org/10.1057/jos.2014.38

Wang, T., Cheng, J., Yang, Y., Esposito, C., Snoussi, H. & Tao, F. (2022). Adaptive Optimization Method in Digital Twin Conveyor Systems via Range-Inspection Control, in IEEE Transactions on Automation Science and Engineering, 19 (2), pp. 1296-1304. https://doi.org/10.1109/TASE.2020.3043393.

Židek, K., Hladký, V., Pitel', J., Demčák, J., Hošovský, A. & Lazorík, P. (2021). SMART Production System with Full Digitalization for Assembly and Inspection in Concept of Industry 4.0. In: Lecture Notes of the Institute for Computer Sciences, Social Informatics and Telecommunications Engineering, vol 382. Springer, Cham. https://doi.org/10.1007/978-3-030-78459-1_13

Technologia i Automatyzacja Montażu

Volume 123, Issue 1/2024, Pages 23-29
https://doi.org/10.7862/tiam.2024.1.4

Original Research

EFFECT OF TIBW ANTI-WEAR COATING ON CUTTING TOOLS FOR MILLING OF NICKEL ALLOYS ON TOOL WEAR AND INTEGRITY OF STATE OF THE TECHNOLOGICAL SURFACE LAYER

WPŁYW POWŁOKI PRZECIWZUŻYCIOWEJ TIBW NA FREZACH DO OBRÓBKI STOPÓW NIKLU NA ZUŻYCIE NARZĘDZIA ORAZ STAN TECHNOLOGICZNEJ WARSTWY WIERZCHNIEJ

Witold HABRAT[1,*], Jarosław TYMCZYSZYN[1], Anna SKROBAN[2], Nikolaos KARKALOS[3]

[1] Rzeszów University of Technology, Faculty of Mechanical Engineering and Aeronautics, al. Powstańców Warszawy 8, 35-959 Rzeszów, Poland
[2] BRYK Sp. z o.o., 36-002 Jasionka 954H, Poland
[3] National Technical University of Athens, School of Mechanical Engineering, 15780 Zografou, Greece

* Corresponding author: witekhab@prz.edu.pl, tel.: +48 17 865 1491

Abstract

In the article, research was carried out to determine the impact of the TiBW anti-wear coating on the operational properties of cutting tools for machining nickel alloys. The dynamics of tool wear were determined on the basis of changes in the components of the total cutting force, microscopic observation of wear on the flank surface, and observation of wear based on SEM images. The condition of the technological surface layer was also determined in the form of changes in the microstructure morphology and hardening of the surface layer. The research was compared to a reference tool with the same geometry with an AlTiN coating. It was shown, among other things, that TiBW coatings can be used successfully for cutting tools for machining nickel alloys, and that the wear dynamics is similar to those of tools with the AlTiN coating. The analyses confirmed the significant thermomechanical impact of the cutter during machining, manifested by chipping and a tendency to strengthen the processed material. On the basis of observations of the microstructure of the surface layer after processing, it was shown that the thermal conductivity of the TiBW coating may be lower than that of the AlTiN coating, which is reflected in the different depths of the thermomechanical interaction zones.

Keywords: anti-wear coatings, TiBW, milling, nickel alloys, surface layer

Streszczenie

W ramach przeprowadzonych badan określono wpływ powłoki przeciwzużyciowej TiBW na właściwości eksploatacyjne narzędzi skrawających do obróbki stopów niklu. Określono przy tym dynamikę zużycia narzędzia na podstawie zmian składowych całkowitej siły skrawania, obserwacji mikroskopowej zużycia na powierzchni przyłożenia oraz obserwację zużycia n podstawie obrazów SEM. Określono również stan technologicznej warstwy wierzchniej w postaci zmian morfologii mikrostruktury oraz utwardzenia warstwy przypowierzchniowej. Badania odniesiono do narzędzia referencyjnego o tej samej geometrii z powłoką AlTiN. Wykazano m.in., że powłoki TiBW mogą być z powodzeniem stosowane na narzędzia skrawające do obróbki stopów niklu a dynamiki zużycia jest podobna do narzędzi z powłoką AlTiN. Analizy potwierdziły istotne oddziaływanie termo-mechaniczne freza podczas obróbki objawiające się wykruszeniami oraz tendencją do umocnienia materiału obrabianego. Na podstawie obserwacji mikrostruktury warstwy wierzchniej po obróbce wykazano, że przewodność cieplna powłoki TiBW może być mniejsza niż w przypadku powłoki AlTiN, co objawia się w różnej głębokości stref oddziaływań termo-mechanicznych.

Słowa kluczowe: powłoki przeciwzużyciowe, TiBW, frezowanie, stopy niklu, warstwa wierzchnia

This is an Open Access article distributed under the terms of the Creative Commons Attribution License CC BY 4.0 (https://creativecommons.org/licenses/by/4.0/)

1. Introduction

Cutting tools are fundamental elements of machining processes in order to remove material for the final desired shape of mechanical parts to be created. A wide variety of cutting tools exist, depending on the machining process and specific operation such as turning inserts, end mills, or drills. Tool wear constitutes a significant problem for cutting tools and an important component of machining cost as well. Thus, appropriate coatings are often applied to cutting tools as a means of improving their performance and extending their service life by protecting them from the influence of friction and intense heat produced during machining.

Especially, when difficult-to-cut materials such as nickel superalloys are machined, it is anticipated that tool wear can be excessive, radically shortening the tool life, unless specially designed coatings or cooling strategies are employed (Buddaraju et al., 2021; Paturi et al., 2021). Nickel-based alloys are used in many high-end applications such as in the aerospace industry as they possess properties such as high hardness, high resistance to corrosion and creep, as well as poor thermal conductivity and tendency to high strain hardening (Buddaraju et al., 2021; Parida & Maity, 2018; Paturi et al., 2021; Pedroso et al., 2023). Thus, machining of these alloys can cause high tool wear rate, with different wear mechanisms occurring such as adhesion, oxidation, abrasion, debonding and diffusion (Pedroso et al., 2023). In order to overcome the problem of high wear rate, cutting tools for machining nickel alloys should have high strength and toughness, high thermo-chemical stability and thermal shock resistance (De Bartolomeis et al., 2021). For that reason specific categories of tools are recommended, such as CBN, ceramic and carbides, with appropriate coatings (De Bartolomeis et al., 2021) or processed with suitable techniques such as chemical-mechanical polishing in order to exhibit superior performance (Tanaka et al., 2022).

As machining of superalloys is nowadays very important in industrial practice, a considerable amount of relevant works has been carried out. For example, Kosaraju, Vijay Kumar and Satish (2018) and Waghmode and Dabade (2019) investigated the impact of process parameters on machining forces and surface quality during machining of nickel-based alloys. Other researchers have focused on the determination of ways to improve the wear resistance of cutting tools or reduce wear rate during machining of nickel-based alloys. Bergs, Hardt and Schraknepper (2020) showed that the cemented carbide grade has a direct influence on tool wear behavior, with submicron or ultrafine grades being superior to conventional ones but the effect on surface quality was minimum. Guimaraes et al. (2023) performed a novel study, presenting the consequences of machining nickel alloys with a worn tool on residual stresses, corrosion, fatigue and surface hardness, clearly indicating that tool wear has a detrimental effect on the workpiece integrity.

Hadi et al. (2013) and Li, Zeng and Chen (2006) proved that milling mode also has an impact of tool wear, as down-milling should be preferred over up-milling. Moreover, the monitoring of cutting forces can be a significant indicator for tool wear. Sørby and Vagnorius (2018) noted that high pressure cooling does not affect tool wear significantly but facilitates chip breaking. Parida and Maity (2018) evaluated the performance of nickel alloy machining under elevated temperatures and observed a notable reduction of forces, roughness and tool wear. Yildirim (2019) compared various advanced cooling methods for enhancing machinability of nickel alloys and determined that the lowest tool wear was obtained by cryo-MQL strategy with nanofluids. Finally, apart from experimental work, some authors such as Parida and Maity (2019) and Lotfi, Jahanbasksh and Farid (2016) performed FE simulations to study subjects relevant to superalloy machining, such as hot machining or tool wear between different types of cutting tools.

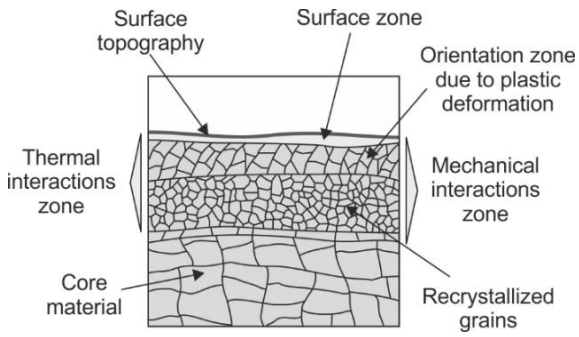

Fig. 1. Structure of the technological surface layer after cutting processes

The application of nickel alloys in aircraft technology brings additional construction requirements to the quality of the final product including the state of the technological surface layer (Fig. 1).

In the present work, an experimental work is carried out to determine the effect of a special TiBW anti-wear coating on tool wear and integrity of machined surfaces during machining of Inconel 718 alloy. For that reason, side milling experiments were carried out under specific conditions, with two different types of coating, and their performance was evaluated by observing cutting force components at different stages of tool wear, as well as by measuring

flank wear and surface hardness. Finally, analysis of the results justified the superiority of the TiBW coating.

2. Material and methods

2.1. Workpiece material

The workpiece material in this study was Inconel 718, which is a high-temperature resistant nickel-based superalloy. The surface of this material exhibited a hardness of approximately 36 HRC.

The chemical composition of Inconel 718 includes several alloying elements as follows: Nickel and Cobalt (Ni+Co) content ranges from 50% to 55%, Chromium (Cr) content varies from 17% to 21%, Iron (Fe) serves as the balance component, Cobalt (Co) constitutes 1%, Molybdenum (Mo) ranges from 2.8% to 3.3%, Niobium and Tantalum (Nb+Ta) content is between 4.75% and 5.5%, Titanium (Ti) ranges from 0.65% to 1.15%, Aluminum (Al) varies from 0.20% to 0.80%, Carbon (C) content is 0.08%, Manganese (Mn) is at 0.35%, Silicon (Si) at 0.35%, Boron (B) at 0.006%, and Copper (Cu) is present at 0.3%.

Typically, the mechanical properties of Inconel 718 exhibit the following mechanical properties under ambient conditions (PN-EN ISO 6892-1:2020-05): a tensile strength of 1240 MPa, an elastic strength (0.2%) of 1036 MPa and Young's modulus of 211 GPa.

This particular nickel-chromium-based superalloy is classified as a precipitation hardening alloy, with austenite as the alloying phase that crystallises in the crystal lattice A1 and serves as the matrix material. Inconel 718 is classified as a difficult to machine material, falling into the group "S" according to ISO standards.

2.2. Cutting tools

Carbide tools for the purposes of the research were manufactured with the use of ultra-micrograin grade CKi®12 (Ihle) with extreme toughness and hardness, thus highly recommended e.g. for machining titanium alloys, heat-resistant alloys, austenitic stainless steels, hardened steels. The geometry of the milling cutter intended for the tests is shown in Fig. 2.

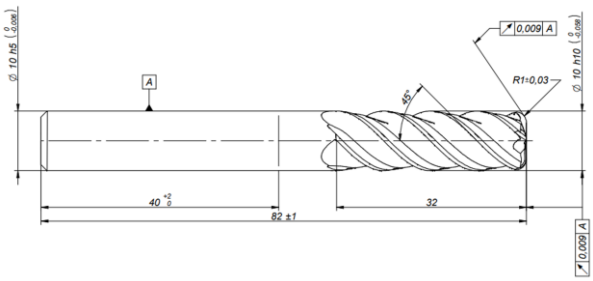

Fig. 2. The geometry of the cutting tool used for tests

The prepared tools were covered with the use of TiBW coating with a thickness of 1.3μm (Fig. 3).

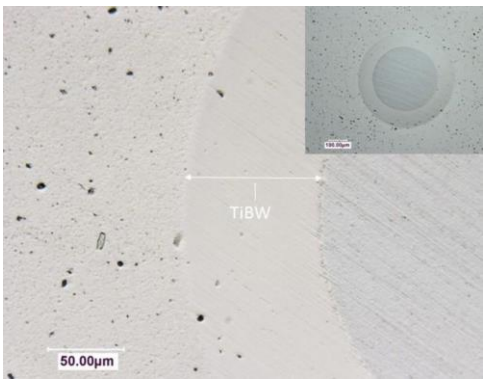

Fig. 3. TiBW coating thickness measurement – ball cratering test

In order to relate the obtained results to commercially available material solutions in terms of improving wear resistance, a reference tool with a commercially available AlTiN coating, commonly used for machining Inconel alloys, was prepared.

2.3. Cutting condition

The tests were carried out on a DMU 80 P duoBlock CNC milling machine (Fig. 4). The test stand was equipped with a Kistler piezoelectric dynamometer with a measuring range of ±5 kN attached to the machine table. The signal from the force meter is transferred to the charge amplifier and transmitted to the computer via the USB port using a 16-bit analog-to-digital converter with a measurement range of ± 10 V. The signal was visualized, processed and saved using a program developed in the LabVIEW environment. The signal sampling frequency was set to 2 kHz.

Fig. 4. Test stands built based on the DMU 80 P duoBlock CNC milling machine

The following cutting parameters were adopted:

- cutting speed v_c = 25 m/min,
- depth of cut a_p = 2 mm,
- cutting width a_e = 2.5 mm,
- feed f = 0.03 mm/tooth.

The microstructure of the surface layer was observed for samples cut from the processed material in the area for blade wear corresponding to the cutting distance L = 150 mm and L = 450 mm. The side surface was observed after the milling process (Fig. 5).

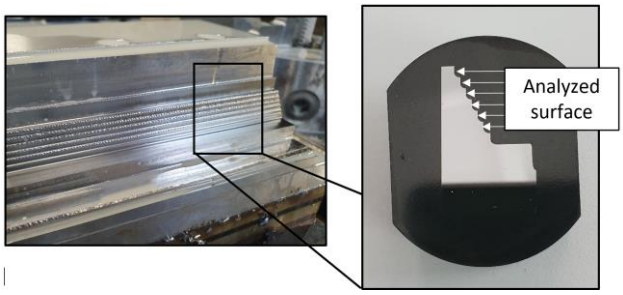

Fig. 5. The analysed side surface after processing

3. Results and discussion

The wear of the cutting tool blade results in a change in the mechanical impact conditions and, consequently, in the components of the total cutting force. Monitoring these forces allowed comparison of the operational wear of the tested and reference tools. The measured components determine the averaged maximum values for the force fluctuations resulting from the cutting of subsequent blades. The Fx component was defined in the feed direction, Fy perpendicular to the feed, and Fz in the axial direction.

The figures below show a graph of changes in the measured components of the total force as a function of the cutting length in relation to the reference tool with the AlTiN coating (Fig. 6) and the cutting tool with the TiBW coating (Fig. 7).

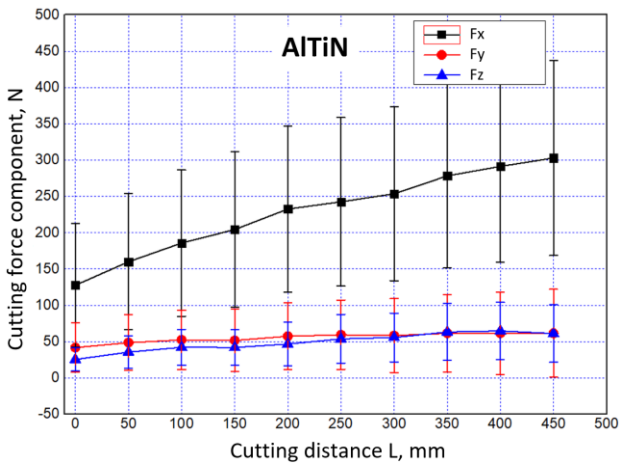

Fig. 6. Graph of changes of the total cutting force components as a result of tool wear as a function of cutting distance up to 450 mm for a cutter with an AlTiN coating

The obtained results show significant similarities in terms of the increase in force of Fx - 134% for the cutter with the AlTiN coating and 125% for the cutter with the TiBW coating. This proves the good functional properties of the tested coating in the milling of nickel superalloys.

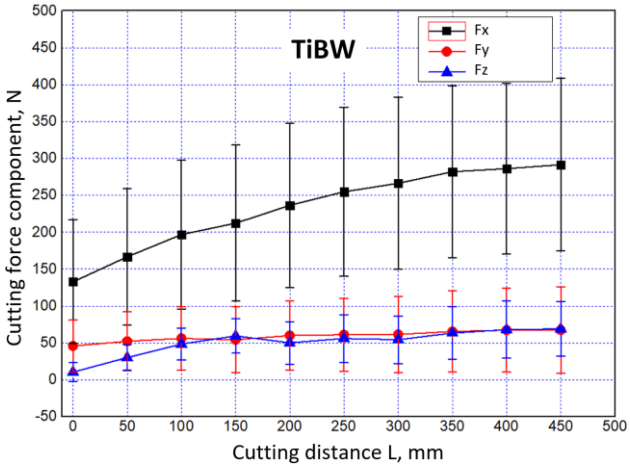

Fig. 7. Graph of changes of the total cutting force components as a result of tool wear as a function of cutting distance up to 450 mm for a cutter with a TiBW coating

The analysis of wear on the tool flank surface after cutting distance 450 mm (approximately 6 min 17 s) also did not show significant differences (Fig. 8).

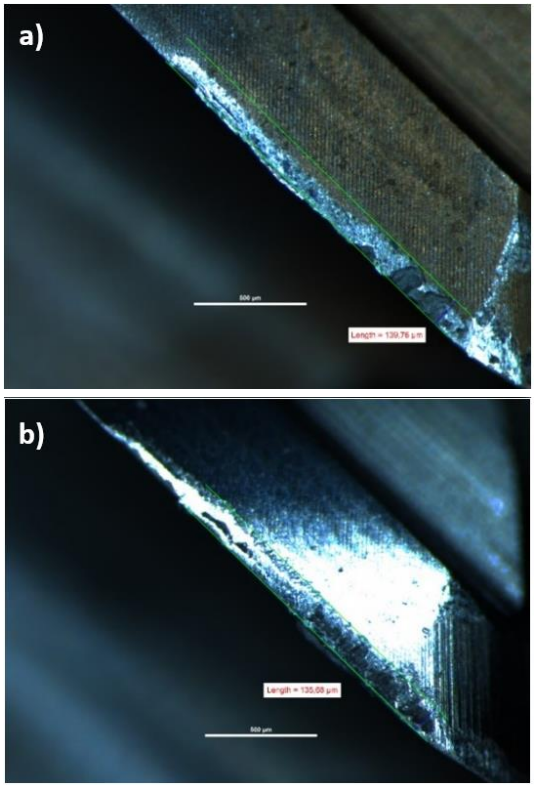

Fig. 8. Wear on the flank surface after cutting 450 mm for a tool with coating a) AlTiN, b) TiBW

Both abrasion and chipping of the blade can be observed. In the case of a tool with a TiBW coating, the chipping area appears to be slightly larger. SEM

analysis of the wear of the cutting edge of the TiBW-coated tool confirmed cracks in the blade, which may be the result of thermomechanical interactions in the cutting zone (Fig. 9). This thesis is confirmed by the analysis of the microstructure of the surface after machining with a tool in the initial and final stages of wear (Fig. 10 and 11).

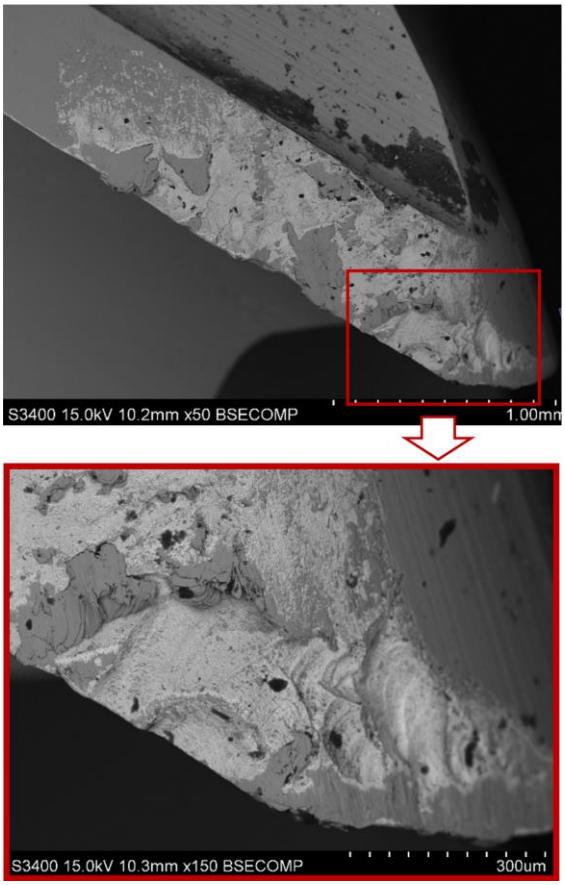

Fig. 9. SEM image of the wear of the cutting edge of a tool with a TiBW coating

In the case of a tool with a TiBW coating, wear significantly increases the thermomechanical influence zone, which can be observed in the form of a longitudinal texture near the machined surface to a depth not exceeding 10 mm (Fig. 10b). This effect was confirmed by the strengthening in the near-surface layer shown in Figure 12. The tendency to be strengthened by large plastic deformations for materials of the HRSA group occurs especially in the case of worn tools. An increase in cutting force due to wear and the influence of heat generated during cutting can cause this type of phenomenon.

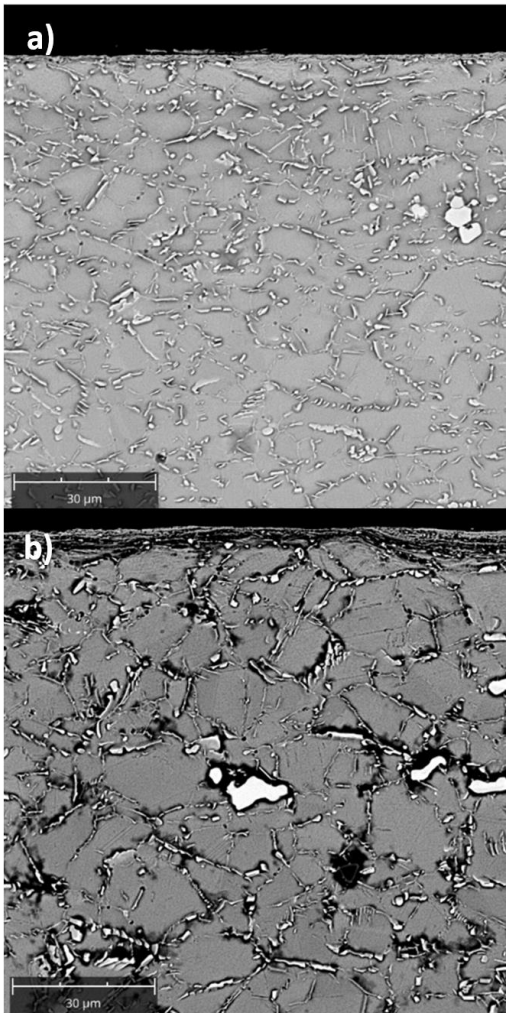

Fig. 10. Comparison of changes in the morphology of the microstructure of the surface layer after machining with a milling cutter with a TiBW coating after cutting: a) 150 mm, b) 450 mm

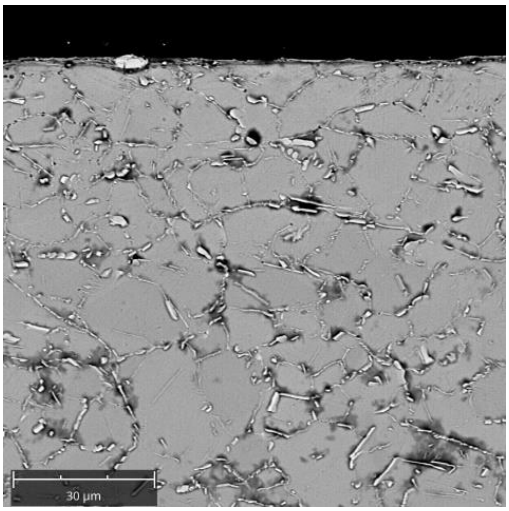

Fig. 11. Comparison of changes in the morphology of the microstructure of the surface layer after machining with a cutter with an AlTiN coating after cutting 450 mm

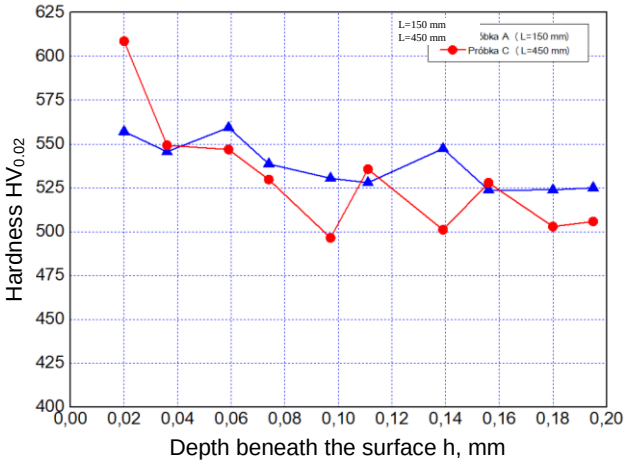

Fig. 12. Hardness distribution in the surface layer after machining with tools in various phases of wear (cutting distance L)

Comparison of changes in the morphology of the microstructure of the surface layer after processing with a worn cutter with a TiBW coating (Fig. 10b) and a cutter with an AlTiN coating (Fig. 11) allow the conclusion that the tested coatings differ from each other in terms of thermal conductivity. The potentially lower thermal conductivity of the TiBW coating causes the heat flow generated in the cutting process to be directed towards the processed material. As a consequence, this creates the above-mentioned zone of influence of thermo-mechanical interactions. However, confirmation of this thesis requires laboratory determination of thermal conductivity coefficients for the analysed coatings.

4. Conclusions

Based on the obtained results, the following conclusions were drawn:

- it was demonstrated that TiBW coatings can be successfully used for cutting tools for machining the Inconel 718 alloy, showing similarity in wear dynamics to commonly used tools with commercially available AlTiN coatings,
- determining the dynamics of wear based on changes in the components of the total cutting force showed that the component in the feed direction is the largest, and its increase over the assumed period of operation (approximately 6 min of cutting) was - 134% for the cutter with an AlTiN coating and 125% for the cutter with the coating TiBW,
- the amount of wear on the flank surface for the analyzed tools did not show significant differences, while for the tool with the TiBW coating a slightly larger area of chipping could be observed,
- SEM analysis of the worn blade and a graph of hardness as a function of depth from the surface confirmed the significant thermo-mechanical impact of the cutter during processing, manifested by chipping and a tendency to strengthen,
- based on observations of the microstructure of the surface layer after processing, it was shown that the thermal conductivity of the TiBW coating may be lower than that of the AlTiN coating. This directs the heat flow generated in the cutting process towards the workpiece material and translates into the depth of deformation. Confirmation of this, however, requires further material and operational tests.

Acknowledgments

Research financed by the project "New cutting tools with innovative anti-wear coatings for machining nickel-based superalloys used in aviation technology" RPPK.01.02.00-18-0020/19 implemented at P.P.U.H. "BRYK" Witold Bryk, 36-002 Jasionka, Jasionka 954

References

Bergs, T., Hardt, M., & Schraknepper, D. (2020). Investigations on the Influence of the Cemented Carbide Grade on the Surface Integrity when End Milling DA 718. *Procedia CIRP*, *93*, 1490–1495. https://doi.org/10.1016/J.PROCIR.2020.03.068.

Buddaraju, K. M., Ravi Kiran Sastry, G., & Kosaraju, S. (2021). A review on turning of Inconel alloys. *Materials Today: Proceedings*, *44*, 2645–2652. https://doi.org/10.1016/J.MATPR.2020.12.673.

De Bartolomeis, A., Newman, S. T., Jawahir, I. S., Biermann, D., & Shokrani, A. (2021). Future research directions in the machining of Inconel 718. In *Journal of Materials Processing Technology* (Vol. 297). Elsevier Ltd. https://doi.org/10.1016/j.jmatprotec.2021.117260.

Guimaraes, M. C. R., Fogagnolo, J. B., Paiva, J. M., Veldhuis, S., & Diniz, A. E. (2023). The impact of the cutting parameters and tool condition on surface integrity when milling Inconel 625. *Journal of Materials Research and Technology*, *25*, 1944–1958. https://doi.org/10.1016/j.jmrt.2023.06.071.

Hadi, M. A., Ghani, J. A., Che Haron, C. H., & Kasim, M. S. (2013). Comparison between up-milling and down-milling operations on tool wear in milling Inconel 718. *Procedia Engineering*, *68*, 647–653. https://doi.org/10.1016/j.proeng.2013.12.234.

Kosaraju, S., Vijay Kumar, M., & Sateesh, N. (2018). Optimization of Machining Parameter in Turning Inconel 625. *Materials Today: Proceedings*, *5*(2), 5343–5348. https://doi.org/10.1016/j.matpr.2017.12.119.

Li, H. Z., Zeng, H., & Chen, X. Q. (2006). An experimental study of tool wear and cutting force variation in the end milling of Inconel 718 with coated carbide inserts. *Journal of Materials Processing Technology*, *180*(1–3), 296–304. https://doi.org/10.1016/j.jmatprotec.2006.07.009.

Lotfi, M., Jahanbakhsh, M., & Akhavan Farid, A. (2016). Wear estimation of ceramic and coated carbide tools in turning of Inconel 625: 3D FE analysis. *Tribology International*, *99*, 107–116. https://doi.org/10.1016/j.triboint.2016.03.008.

Parida, A. K., & Maity, K. (2018). Comparison the machinability of Inconel 718, Inconel 625 and Monel 400 in hot turning operation. *Engineering Science and Technology, an International Journal*, *21*(3), 364–370. https://doi.org/10.1016/j.jestch.2018.03.018.

Parida, A. K., & Maity, K. (2019). FEM analysis and experimental investigation of force and chip formation on hot turning of Inconel 625. *Defence Technology*, *15*(6), 853–860. https://doi.org/10.1016/j.dt.2019.04.012.

Paturi, U. M. R., B., V. D., & Reddy, N. S. (2021). Progress of machinability on the machining of Inconel 718: A comprehensive review on the perception of cleaner machining. *Cleaner Engineering and Technology*, *5*, 100323. https://doi.org/10.1016/J.CLET.2021.100323.

Pedroso, A. F. V., Sousa, V. F. C., Sebbe, N. P. V., Silva, F. J. G., Campilho, R. D. S. G., Sales-Contini, R. C. M., & Jesus, A. M. P. (2023). A Comprehensive Review on the Conventional and Non-Conventional Machining and Tool-Wear Mechanisms of INCONEL®. In *Metals* (Vol. 13, Issue 3). MDPI. https://doi.org/10.3390/met13030585.

Sørby, K., & Vagnorius, Z. (2018). High-pressure cooling in turning of inconel 625 with ceramic cutting tools. *Procedia CIRP*, *77*, 74–77. https://doi.org/10.1016/j.procir.2018.08.221.

Tanaka, Y., Sato, H., & Eryu, O. (2022). Improved cemented carbide tool edge formed by solid phase chemical–mechanical polishing. *Journal of Materials Research and Technology*, *20*, 606–615. https://doi.org/10.1016/J.JMRT.2022.07.077.

Waghmode, S. P., & Dabade, U. A. (2019). Optimization of process parameters during turning of Inconel 625. *Materials Today: Proceedings*, *19*, 823–826. https://doi.org/10.1016/j.matpr.2019.08.138.

Yıldırım, Ç. V. (2019). Experimental comparison of the performance of nanofluids, cryogenic and hybrid cooling in turning of Inconel 625. *Tribology International*, *137*, 366–378. https://doi.org/10.1016/J.TRIBOINT.2019.05.014.

Technologia i Automatyzacja Montażu

Volume 123, Issue 1/2024, Pages 30-36
https://doi.org/10.7862/tiam.2024.1.5

Original Research

SIMULATION BASED STUDY OF GROUND MOBILE ROBOTS FOR INSPECTION AND CONTROL OF THE BRIDGE ASSEMBLY PROCESS

BADANIE OPARTE NA SYMULACJI NAZIEMNYCH ROBOTÓW MOBILNYCH DO INSPEKCJI I KONTROLI PROCESU MONTAŻU MOSTU

Pierluigi REA[1], Erika OTTAVIANO[2], Lucia FIGULI[3,*]

[1] Dept. of Mechanical, Chem. and Materials Eng., University of Cagliari, Via Marengo 2, 09123 Cagliari, Italy
[2] Dept. of Civil and Mech. Eng., University of Cassino, via DI Biasio 43, 03043, Cassino (FR), Italy
[3] Faculty of Security Engineering, University of Zilina, Univerzitna 8215/1, 01026 Zilina, Slovakia

* Corresponding author: pierluigi.rea@unica.it

Abstract

Nowadays, the inspection of bridges poses a significant challenge for safeguarding critical infrastructures. Recent advancements have seen the integration of robots to replace human personnel in hazardous tasks. These robots, whether operating autonomously or through tele-operation, play a crucial role in monitoring structures and infrastructure, ensuring secure access to areas such as manholes on decks and box girder bridges. Specifically designed for environments deemed dangerous, difficult, or inaccessible to humans, ground mobile robots equipped with appropriate sensors are increasingly deployed for inspection purposes. This paper addresses simulation tests conducted by a hybrid mobile robot. Its compact design and maneuverability enable it to navigate through obstacles, making it suitable for inspecting railway or highway bridge decks as well as confined spaces within box girder bridges. The study includes a survey of existing bridges highlighting key issues to be addressed and presents simulation results for the hybrid rover. Automatic and robotic systems can play an important role for the control during the bridge assembling process increasing the reliability of the structure and improving its operational properties and security.

Keywords: Ground Mobile Robots, Bridge Inspection, Simulation, Structural Health Monitoring

Streszczenie

Obecnie inspekcje mostów stanowią istotne wyzwanie dla ochrony infrastruktury krytycznej. Najnowsze osiągnięcia umożliwiły integrację robotów w celu zastąpienia personelu ludzkiego przy wykonywaniu niebezpiecznych zadań. Roboty te, działające autonomicznie lub w trybie teleoperacji, odgrywają kluczową rolę w monitorowaniu konstrukcji i infrastruktury, zapewniając bezpieczny dostęp do takich obszarów, jak włazy na pokładach i mosty z dźwigarami skrzynkowymi. Zaprojektowane specjalnie dla środowisk uznawanych za niebezpieczne, trudne lub niedostępne dla człowieka, naziemne roboty mobilne wyposażone w odpowiednie czujniki są coraz częściej wykorzystywane do celów inspekcyjnych. W artykule omówiono badania symulacyjne prowadzone przez hybrydowego robota mobilnego. Jego zwarta konstrukcja i zwrotność umożliwiają mu pokonywanie przeszkód, dzięki czemu nadaje się do inspekcji pomostów kolejowych lub autostradowych, a także ograniczonych przestrzeni w mostach z dźwigarami skrzynkowymi. Badanie obejmuje przegląd istniejących mostów, podkreślając kluczowe problemy, którymi należy się zająć, i przedstawia wyniki symulacji dla łazika hybrydowego. Systemy automatyczne i zrobotyzowane mogą odegrać ważną rolę w sterowaniu procesem montażu mostu, zwiększając niezawodność konstrukcji oraz poprawiając jej właściwości eksploatacyjne i bezpieczeństwo.

Słowa kluczowe: Naziemne roboty mobilne, inspekcje mostów, symulacja, monitorowanie stanu konstrukcji

This is an Open Access article distributed under the terms of the Creative Commons Attribution License CC BY 4.0 (https://creativecommons.org/licenses/by/4.0/)

1. Introduction

Robotics and automation play an important role for many applications. Traditionally developed for industrial tasks, such as pick and place, welding, spraying, deburring, just to cite some, robots have been used in a wide range of different domains, such as, service (Sprenger and Mettler, 2015), remote exploration (Shapovalov and Pereira, 2020), agriculture (Acaccia et al., 2003)), and inspection (Ottaviano et al., 2014; Rea and Ottaviano, 2023).

Referring to the inspection of structures and infrastructure, the use of automatic or teleoperated systems allows increasing safety of the operation, reduce time and cost of survey and thus make the process more systematic and prone to be used for preventing critical damages or structural collapses. Moreover, the use of automatic systems allows collecting data from several sensors making the inspection task repeatable and safe.

Referring to infrastructure inspection, the use of Unmanned Aerial Vehicles (UAV) has enormously increased because of their main characteristics, namely wireless transmission, rapid and cost-effective deployment. Recently, the level of autonomy, which was the main drawback, has been enlarged (Amici et al., 2021). Although their advantages and leading role in outdoor inspections, when dealing with confined spaces, pipelines, box girder bridges and in all cases of harsh environments conditions or heavy payloads, alternatives must be considered.

Ground Mobile Robots (GMR) are a type of Unmanned Ground Vehicles (UGV) that are used in combination with or as alternative of UAVs. They can be classified according to the locomotion type; therefore, they can use wheels (Rajendran et al., 2022), legs (ANYbotics, 2024), tracks (Sahari et al., 2022) or combinations of the previous types (Ottaviano and Rea, 2013), the latter are named as hybrid mobile robots.

Wheeled robots are the most common ones, they are robust and energy saving systems, the main drawback is related to the environment, they are effective in almost flat surfaces, being able of overpassing obstacles of limited size. Legged robots have been developed to overcome these limitations, being versatile systems, capable also of climbing slopes and stairs in all kinds of environments. Challenges in their use are related to energy consumption, complexity in control and high costs. Finally, hybrid mobile robots have been developed to conjugate obstacle overpassing capability but maintaining complexity of control and costs limited.

In this paper we are presenting a hybrid mobile rover that was developed for inspection purposes. In particular, we have chosen two different types of bridges to simulate the behavior of hybrid mobile robot in the survey, demonstrating its ability in negotiating different scenarios.

2. Bridge Inspection

Following the bridge collapse in Genoa, Italy, on 14 August 2018, which resulted in the deaths of 43 people, the scientific and professional community has begun to focus intensively on the poor condition of bridge structures. These scientific and professional activities are being addressed both in Italy and in Slovakia. The bridge over Polcevera, or otherwise known as the Morandi Bridge, was put into operation in 1967 after 4 years of construction. The longest span of the bridge structure was 210 m, the total length: 1182 m, and with a pylon height of 90 m, built as prestressed reinforced concrete, it was the top work of the time, named after the designer Riccardo Morandi. An extensive investigation confirmed that the bridge's collapse was due to a lack of maintenance.

The current state of bridge structures in road and rail transport in Slovakia is alarming. This is evidenced not only by the collapsed bridges in the Slovak Republic (Spišská Nová Ves bridge, bridge in Trstena over the Oravica river bridge over the Turiec river, bridge over the Hornád river, but also by the alarming condition of many other bridge constructions. For example, those that had to be closed immediately, because in the process of their reconstruction it was found that their condition was significantly worse than expected. Therefore, a much more complex reconstruction or their removal and the construction of a new bridge (e.g. the bridge in Hlohovec, the Podtureň bridge, etc.) is needed.

In Italy the situation is similar, high number of collapsed bridges demonstrates the gravity of the situation.

In the Slovak Republic, the use of new more modern technologies for bridge diagnostics is lagging. Long-term monitoring of bridges is exceptional in the environment of ŽSR (Slovak railways) and encounters a significant problem with the analysis and evaluation of a large amount of data. A comprehensive Bridge Management System (BMS) has been introduced abroad, which is a means of managing bridges during the so-called life cycle of the object, i.e. from design, construction, operation to maintenance of bridges. In Italy for road bridges was established a new industrial plan for years 2016-2020, where new inspection procedures were defined, and Bridge Management System (BMS) realized (Figuli et al. 2021).

3. Ground Mobile Robot for Bridge Inspection

In this paper a ground mobile rover is considered, as it is shown in Figures 1 and 2; the mechanical design and its main features have been proposed in (Rea and Ottaviano, 2023). The rover is of hybrid type, since it is designed having tracks commanded by 2 DC motors, and legs commanded by an additional DC motor.

a)

b)

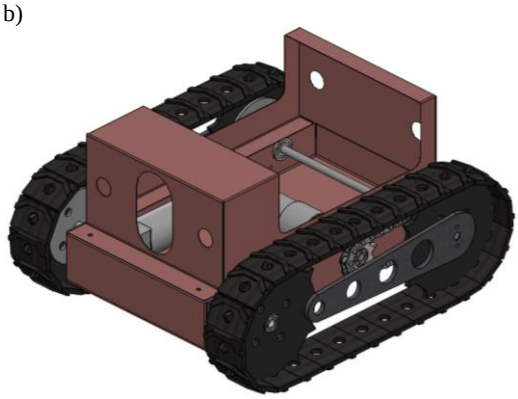

Fig. 1. Ground Mobile Robot: a) a built prototype; b) 3D mechanical design

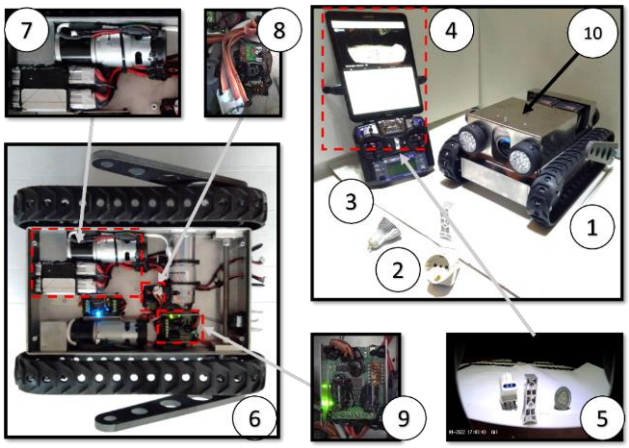

Fig. 2. A scheme of the Ground Mobile Robot: 1) the prototype; 2) objects; 3) Remote Controller; 4) HMI for control; 5) camera view; 6) robot-control boards; 7) motors and battery pack; 8) Spektrum Receiver Mk610; 9) board for control; 10) camera view

Track are used in conjunction with legs when the size of the obstacles to be surpassed is greater than the radius of the tracks.

Figure 2 shows the mechatronic design of the mobile robot, including the HMI (Human Machine Interface) used for teleoperation.

4. Simulation tests

The robot prototype underwent rigorous testing across various operational conditions to assess its engineering viability and performance within real-world scenarios and environments (Rea and Ottaviano, 2023). Specifically, as mentioned earlier, the system underwent testing focused on infrastructure inspection tasks.

4.1. Road Bridges

As road bridges, especially for the important infrastructure, box girder bridges are commonly used worldwide. Box birder bridges are one of types of prestressed bridges. In Slovakia various type of prestressed girders are used for many years and after the years in services the numbers of defects on precast prestressed girder are presented as removed concrete cover, corroded tendons with some ruptured wires, corroded anchors, water leakage through the carriage-way and insulation, overloading of construction, hollow space or voids within concrete caused during casting of the girder, absence of shear reinforcement in prestressed girders, minimal reinforcement ratio was not fulfilled, absence of bonded post-tensioned prestressing, inadequate grouting of tendons and incorrect position of girders on the bearings as is reported in Bujnakova (2017) and Bujnakova (2020). Nowadays another type of box girder bridge is very popular, so called extradosed bridges, number of such types of bridges were constructed lately in Slovakia (Bujňák at al. 2013). For example, a new bridge is in construction in Zilina, over the main railway (see Fig.3). An extradosed bridge combines the main elements of both a prestressed box girder bridge and a cable-stayed bridge. Compared to a cable-stayed, an extradosed bridge uses much shorter pylons than the cable-stayed bridge, and a significantly shallower deck/girder structure than used on the girder bridge. Like any bridge structure, extradosed bridges require regular inspection and maintenance to ensure their long-term performance and safety. Accessing and inspecting the cables and other components of the bridge may pose challenges and require specialized equipment or techniques. The construction of extra-dosed bridges can be more challenging and bring more critical situation. The integration of cables and prestressed concrete elements requires precise coordi-nation and careful execution during construction.

Simulation tests were performed by considering an example of box girder bridge in Fig. 4. The simulation was performed inside the closed elements in the lateral parts in which the floor is inclined. Usually, internal stiffeners are used to reinforce the structure, these elements are considered as obstacles that the robot as to surpass, as it is reported in the numerical simulations of Figs. 5 to 7. Figure 5 shows the motion sequence in which it is necessary to use legs for overpassing the obstacle (the legs are used as propulsive elements). Figs. 6 and 7 reports the actuation for the tracks and legs and kinematic characteristics in terms of velocities and accelerations of the robot center of gravity.

Fig. 3. Box girder bridge: extradosed bridge in Zilina

a)

b)

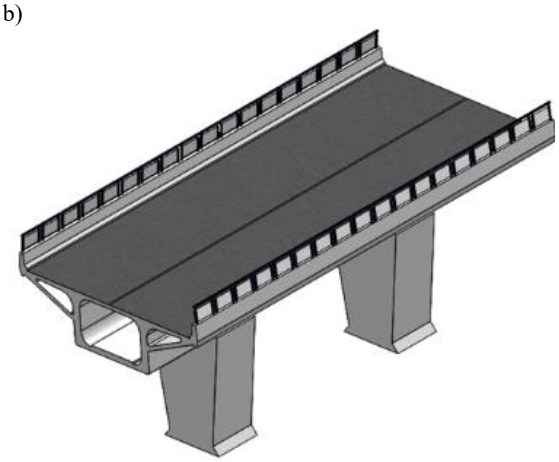

Fig. 4. Box girder bridge example: a) built structure; b) a designed 3D CAD

a)

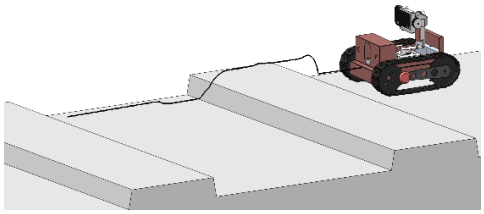

b)

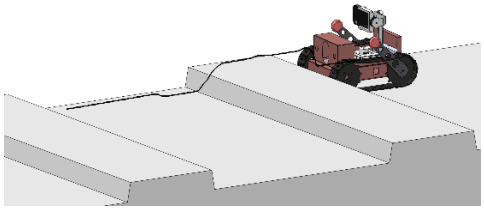

c)

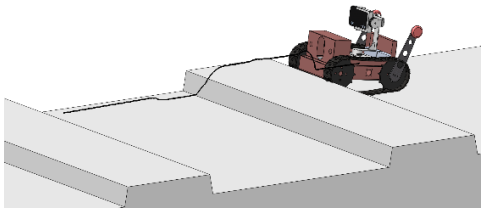

d)

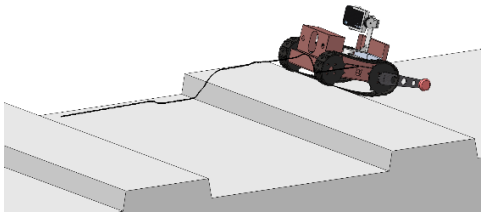

e)

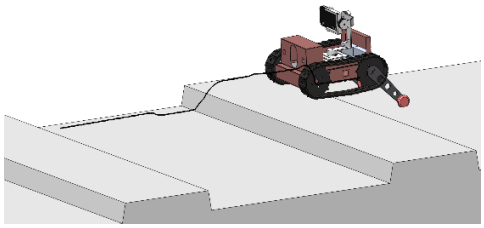

f)

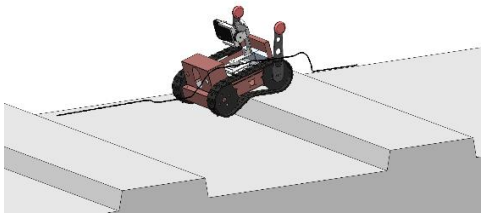

g)

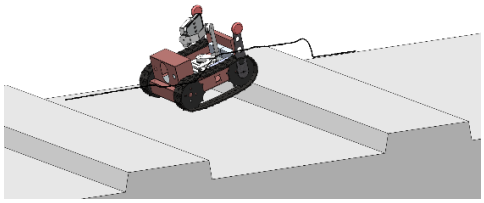

h)

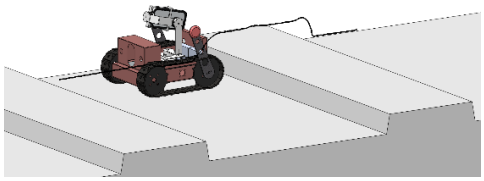

Fig. 5. Motion sequence of the ground mobile robot moving in the box girder bridge

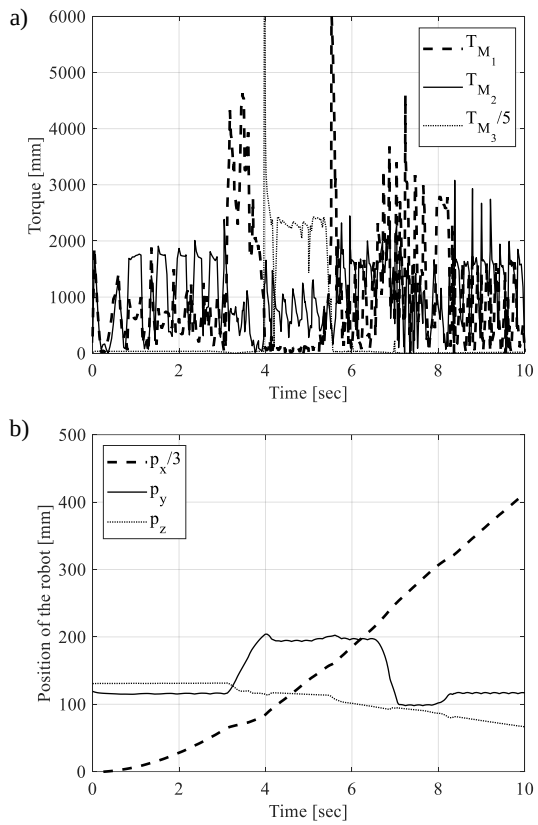

Fig. 6. Simulation results for Figure 5: a) torques for the left and right motors (M_1 and M_2) and legs (M_3); b) coordinates PCM of the center of mass (CM)

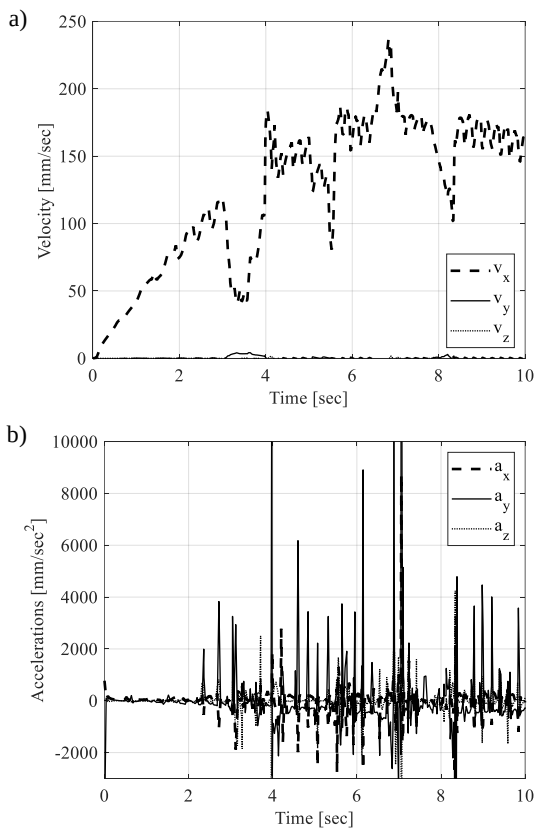

Fig. 7. Results of Figure 5 COM: a) velocities v_x v_y v_z; b) accelerations a_x a_y a_z

4.2. Railway Bridges

Railway bridges are crucial components of railway networks, occupying strategic positions within transportation infrastructure. Over years of use, these structures are subjected to various degradation processes and external influences. Consequently, their durability and reliability diminish over time as a result of these effects (Vičan, J et. al 2015, 2016).

There are 2301 bridges with a total length of 51216 metres registered in railway transport. The average age of railway bridges is more than 60 years. Existing structures need to be inspected to detect any damage and to plan their maintenance.

In Slovakia the high number of bridges are steel structures, mainly as girder bridges for shorter span and truss bridges and arch bridges of special type – girder bridge stiffened by arch.

The simulation tests were conducted in accordance with the specifications to enable the hybrid rover to navigate across the bridge deck. The primary focus of these tests was to identify and navigate over obstacles, with particular emphasis on the rails, as shown in Fig. 9. Numerical results of the simulation are given in Figs. 10 and 11.

Figure 10 reports the velocity and acceleration of the center of gravity of the rover during the motion, Fig. 11 reports the torques for tracks and legs.

Fig. 8. Railway bridge example: a) built structure; b) a designed 3D CAD

The reported simulations can be used to size the actuation and main parts of the robots during the design or verifying the overthrow avoidance when preparing the survey.

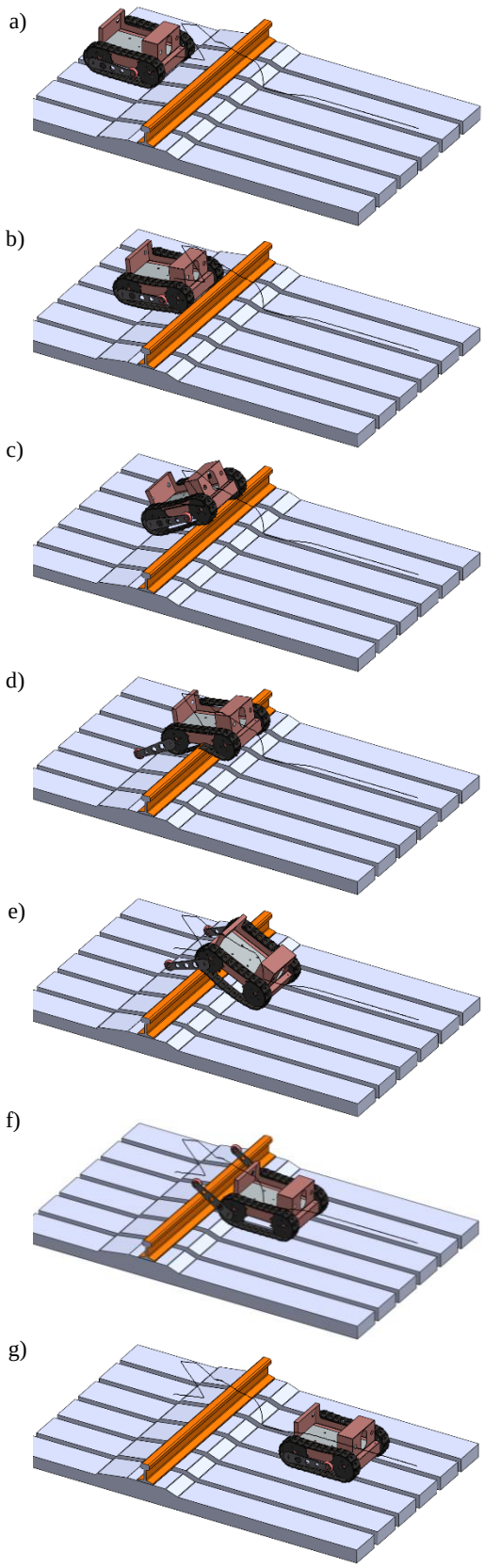

Fig. 9. Motion sequence in the railway bridge

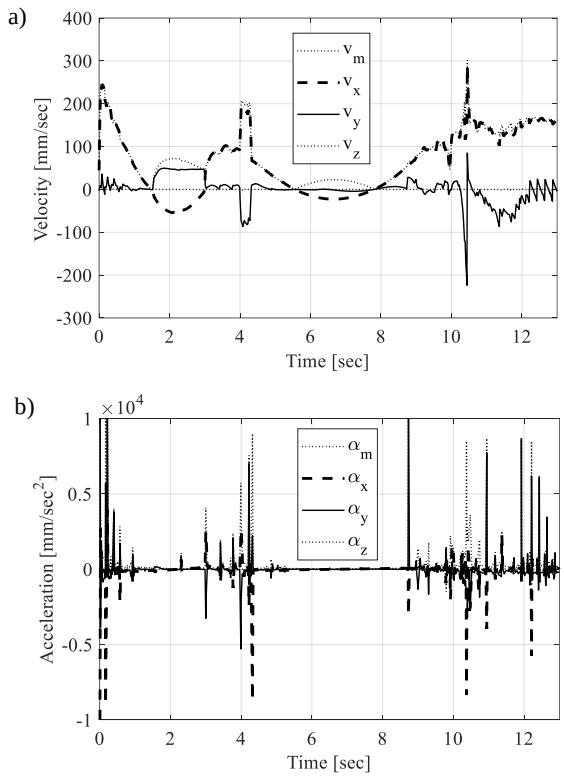

Fig. 10. Results of the simulation in Fig.9: for the center of gravity a) velocity, b) acceleration

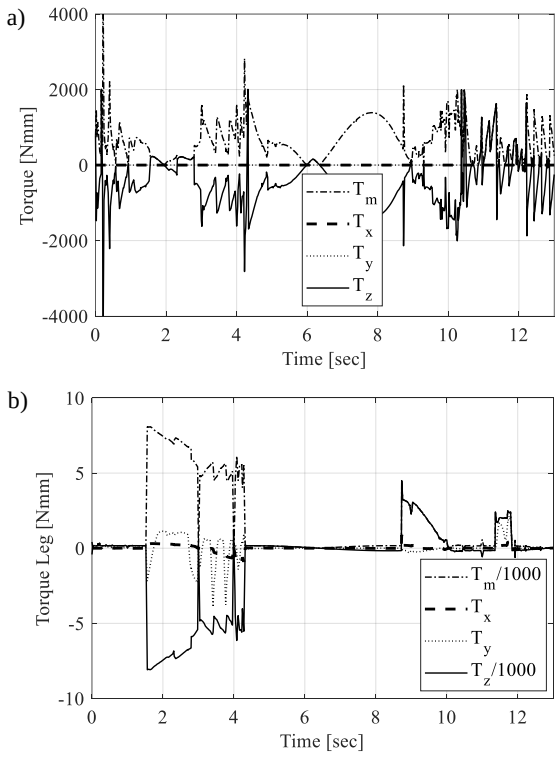

Fig. 11. Results of the simulation in Fig.9: a) torque T_m magnitude and components of tracks; b) for the legs

5. Conclusion

This article proposed the use of ground mobile robots for bridge inspections. In particular, taking into

account two types of bridges structures, having different materials, shapes and problems to face, a built rover has been used for simulating the inspection tasks for planning a survey. Simulation tools and models are widely used to design and optimize the system, but also for preparing and optimizing the inspection tasks before they are executed. It is important to highlight that robots can play an important role also during the bridge assembling process for the control, increasing the reliability of the structure and improving its operational properties and security during operational life. In fact, the ground mobile robots can be autonomous or teleoperated platforms on which materials, sensors, robotic arms for manipulation can be integrated for assembling parts, carrying instruments, installing sensors during the assembly process before and after for inspection and further maintenance.

Acknowledgments

This article is part of a project funded by NATO, Science for Peace and Security Programme Multi-Year Project Application G6001 - MUCADE Multi Cable-Driven Robot for Detecting/Detonating Unexploded Mines and Ordnance.

The article was also supported by The Ministry of Education, Science, Research and Sport of the Slovak Republic and Slovak research and development agency grant number APVV-22-0562 Strengthening the REsilience MAnagement of Key infrastructue Elements using advances in 3D modeling.

References

Acaccia, G.M., Michelini, R.C., Molfino, R.M., Razzoli, R.P. (2003). Mobile robots in greenhouse cultivation: inspection and treatment of plants, *in Proc. of ASER 2003, 1st International Workshop on Advances in Service Robotics*, Bardolino.

ANYbotics website. Available online: https://www.anybotics.com/ (accessed on 25 March 2024).

Amici, C., Ceresoli, F., Pasetti, M., Saponi, M., Tiboni, M., Zanoni, S. (2021). Review of propulsion system design strategies for un-manned aerial vehicles. *Appl. Sci.* 11, 5209. https://doi.org/10.3390/app11115209.

Bujnak, J., Odrobinak, J., Vican, J. (2013). Extradosed Bridge – Theoretical and Experimental Verification, *Procedia Engineering*, Volume 65, pp. 327-334, ISSN 1877-7058, doi:10.1016/j.proeng.2013.09.050.

Bujňáková, P. (2020). Anchorage system in old post-tensioned precast bridges. *Civil and Environmental Engineering*, Volume 16, Issue 2, pp. 379–3871, ISSN 13365835, DOI 10.2478/cee-2020-0038.

Bujňáková, P., Strieška, M. (2017). Development of Precast Concrete Bridges during the last 50 Years in Slovakia. *Procedia Engineering*, 192, pp. 75–79, doi: 10.1016/j.proeng.2017.06.013.

Figuli, L., Gattulli, V., Hoterova, K., Ottaviano, E. (2021). Recent developments on inspection procedures for infrastructure using UAVs. Modern Technologies Enabling Safe and Secure UAV Operation in Urban Airspace, pp. 21–31, ISBN 978-164368189-4, 978-164368188-7, DOI 10.3233/NICSP210003.

Nový cestný nadjazd na Ulici 1. mája v Žiline (2018), ASB.

https://www.asb.sk/stavebnictvo/novy-cestny-nadjazd-na-ulici-1-maja-v-ziline.

Ottaviano, E., Rea, P. (2013). Design and operation of a 2-DOF leg-wheel hybrid robot. *Robotica*, Vol. 31, pp. 1319––1325.

Ottaviano, E., Rea, P., Castelli, G. (2014). THROO: a Tracked Hybrid Rover to Overpass Obstacles. *Advanced Robotics*, Vol. 28, no. 10, doi=10.1080/01691864.2014.891949 (2014).

Rea, P., Ottaviano, E. (2923). Hybrid Inspection Robot for Indoor and Outdoor Surveys. *Actuators 2023*, Vol. 12, No. 108. https://doi.org/10.3390/act12030108.

Rajendran, S. E., Dinakaran, D., Ramanathan, K. C., Ramya, MM, Samuel D.G., Harris. (2022). A Review on Wheeled Type In-Pipe Inspection Robot. Vol. 11. pp. 745–754. 10.18178/ijmerr.11.10.745-754.

Sahari, E., Lai, W., Pulles, A., Guo, XQ., Bernhard, M. (2022). Design and Development of a Tracked Inspection Robot. 10.48550/arXiv.2209.00329.

Shapovalov, D., Pereira, G.A.S. (2020). Tangle-Free Exploration with a Tethered Mobile Robot. *Remote Sens.*, Volume 12, https://doi.org/10.3390/rs12233858.

Sprenger, M., Mettler, T. (2015). Service Robots, Business & Information Systems Engineering, DOI: 10.1007/s12599-015-0.

Vičan, J., Gocál, J., Odrobiňák, J., Koteš, P. (2016). Analysis of Existing Steel Railway Bridges. *Procedia Engineering*, Vol. 156, pp. 507-514. doi: 10.1016/j.proeng.2016.08.328.

Vican, J., Gocal, J., Odrobinak, J., Moravcik, M., Kotes, P. (2015). Determination of railway bridges loading capacity. *Procedia Engineering*, Vol. 111, pp. 839–844.

Technologia i Automatyzacja Montażu

Volume 123, Issue 1/2024, Pages 37-45
https://doi.org/10.7862/tiam.2024.1.6

Original Research

DEVELOPMENT OF A BASIC CAM PROCESSOR FOR A COLLABORATIVE ROBOT FOR WORKSHOP AUTOMATION

OPRACOWANIE PODSTAWOWEGO PROCESORA CAM DLA ROBOTA WSPÓŁPRACUJĄCEGO NA POTRZEBY AUTOMATYZACJI PRAC WARSZTATOWYCH

Andrzej CHMIELOWIEC[1,*], Karol ŁYSIAK[1], Jindřich VILIŠ[2]

[1] Faculty of Mechanics and Technology, Rzeszow University of Technology, Kwiatkowskiego 4, Stalowa Wola, Poland
[2] Department of Mechanical Engineering, Faculty of Military Technology, University of Defence, Kounicova 65, Brno, Czech Republic

* Corresponding author: achmie@prz.edu.pl

Abstract

The article presents an algorithm for constructing a tool path for a collaborative robot. This topic is significant due to the increasing popularity and prevalence of collaborative robots, alongside the lack of software for rapid path generation based on CAD models. Since the dynamics and control of a collaborative robot significantly differ from those of industrial robots and CNC machines, it is necessary to apply an approach that considers the limitations of the cobot. Beyond the tool path construction algorithm itself, the article presents the results of experiments carried out on an actual robot using a programmed CAM processor.

Keywords: collaborative robot, CAM, path generation, workshop automation

Streszczenie

Artykuł prezentuje algorytm tworzenia ścieżki narzędzia dla robota współpracującego. Temat ten jest bardzo istotny ze względu na rosnące rozpowszechnienie tego rodzaju robotów przy jednoczesnym braku oprogramowania pozwalającego na efektywne tworzenie ścieżki ruchu na podstawie modeli CAD. Ponieważ dynamika oraz system sterowania robota współpracującego znacznie różnią się od tych stosowanych w robotach przemysłowych i maszynach CNC, to konieczne jest zastosowanie podejścia dedykowanego kobotom. Poza algorytmem tworzenia ścieżki narzędzia artykuł prezentuje wyniki eksperymentów przeprowadzonych na rzeczywistym robocie przy użyciu zaimplementowanego procesora CAM.

Słowa kluczowe: robot współpracujący, robot kolaboracyjny, CAM, generowanie ścieżki, automatyzacja warsztatu

1. Introduction

Nowadays, technological advances and constant innovations in industry are offering new perspectives in the field of automation and robotics. These innovations are becoming a major source of efficiency and precision in manufacturing processes. A fundamental transformation is the gradual transition from conventional three-axis CNC machines to collaborative robots, known as cobots (Weidemann et al. 2023; Matheson et al. 2019). In this context, the question is - how to efficiently convert G-code, which is originally designed for three-axis CNC machines, into instructions capable of being implemented safely and efficiently in a collaborative robot platform? This issue symbolizes the uniting of two different spheres of industrial production. On the one side are traditional CNC machines, while on the other side are modern

This is an Open Access article distributed under the terms of the Creative Commons Attribution License CC BY 4.0 (https://creativecommons.org/licenses/by/4.0/)

cobots that offer the dynamics, flexibility and the ability to safety interact with human operators to the industrial system (Matheson et al. 2019).

Numerically controlled machine tools, or CNC machines, operate based on coded program instructions, allowing materials to be processed according to strict specifications (Suh et al. 2008). They eliminate the necessary direct manual control of operations. They operate with precisely defined trajectories within fixed workspaces. Trajectory planning on CNC machines is usually controlled by a geometric model created in CAD software (Suh et al. 2008; Ali and Mohsin 2021). The program instructions are passed to the CNC machine in the form of a sequential program that controls the machine behavior, mainly through G-codes. G-codes contain detailed information about the exact positions, feed rates, cutting depth and other parameters that affect the actual machining process (Suh et al. 2008; Ali and Mohsin 2021; Gayathri et al. 2022; Abd Rahman et al. 2023). There are many user interfaces and control programs for CNC machines, but most of them work with vector data (Khan, Shukla, and Singh 2018). For the cutting operations such as milling or turning, M-codes are also used to control the mechanisms of the machine tool (Suh et al. 2008). These M-codes control cooling fluid pumps, signalizing the need for tool changes and providing information about other modular functions. These machines were designed for accurate, repetitive and effective machining of materials. Their main disadvantage is the strict separation of the work area from human operators (Suh et al. 2008; Ali and Mohsin 2021; Gayathri et al. 2022; Abd Rahman et al. 2023; Khan, Shukla, and Singh 2018; Kheirabadi et al. 2023).

One of the possibilities is the use of collaborative robots (Kheirabadi et al. 2023). They are conceptualized with the primary purpose of collaboration and their design reflects the ability to synchronize with human workers. Their main goal is to efficiently perform the tasks that demonstrate high physical and exhaustive character (Berx, Decré, and Pintelon 2024; Chutima 2023; Jocelyn et al. 2023). Specifically, these tasks require high precision in a restricted space, such as precise manipulation of small components or accurate assembly (Hu 2023). For trajectory conversion for cobots, special attention is focused on safety aspects. Trajectory adjustments are necessary to eliminate potential risk of injury, which requires careful trajectory correction with regard to the cobot's ability to operate in the space which is shared with human operators (Toledano-García et al. 2023). The preparation of trajectories emphasizes user-friendly programming that allows quick and intuitive task setup for rapid response to dynamically changing challenges (Toledano-García et al. 2023; Faulwasser et al. 2016; Khoramshahi and Billard 2019). In this context, there is a need for the development of a CAM processor specifically designed for cobots to enable intuitive programming and customization of work trajectories without deep programming knowledge.

Several authors and scientific researchers are increasingly focusing on this innovative area, trying to understand the complex aspects involved in integrating cobots into the work environment. In a review of the evaluation of intelligent collaborative robots, Da Silva et al. (Da Silva et al. 2023) discussed the potential of CAD models for simulating realistic scenarios. They emphasized that simulation using CAD models allowed realistic testing of cobot behavior and was effective for prototype validation. However, simulation can be limited in some situations, especially during validation, so the authors recommend using CAD models in combination with other testing methods for comprehensive performance evaluation. In the study (Parsa and Saadat 2021), authors Soran Parsa and Mozafar Saadat focused on the utilization of CAD models to optimize disassembly planning for end-of-life products. Their goal was to combine human flexibility with robot precision to improve the efficiency of disassembly operations. The work resulted in the disassembly planning method that uses CAD models to identify and prioritize components for reusability. Nagata et al. (Nagata et al. 2013) developed the robotic CAM system for the RV1A industrial robot. This system allows the move of the robot according to tool position and orientation data without using a robot language and it serves as an interface between a conventional CAD/CAM system and an industrial robot. Through the collaboration between the main processor of the CAD/CAM system, the robotic servo controller, and the robot kinematics, the post-processing and learning process for generating robot languages was streamlined. Experimental results demonstrated that the system was able to successfully control robot motion based on tool position and orientation data.

The main goal of this study is to develop a user-friendly tool that enables intuitive trajectory programming for the HCR5 collaborative robot. The result will be the method of converting contours in a three-dimensional CAD model into instructions suitable for the HCR5 collaborative robot. In this way, we expect that the development of the CAM processor will improve the flexibility of approaches to automation in manufacturing, which will increase the efficiency of cobot implementation in industrial operations, and this will ultimately lead to optimization of manufacturing processes and an increase the total productivity.

2. Materials and Methods

Based on the CAD model, it is possible to generate a mesh representing curves, surfaces, and volumes. Curves are one-dimensional objects whose definition does not require significant memory and computational resources. However, curves themselves do not contain information about normal vectors to the surface on which they are located. A different situation arises in the case of a surface mesh, which provides the possibility of accurately determining normal vectors. In this section, conditions for the correct reconstruction of normal vectors based on the curve mesh and methods for their reconstruction based on the surface mesh will be presented.

The selected components of the CAD model were transformed into computational meshes, including both one-dimensional and two-dimensional types, using the open-source Gmsh software (Geuzaine and Remacle 2009). In Fig. 1, an example of a CAD model (blue outline) covered with a mesh of varying density (black and gray lines) is presented. The meshio library, designed for the Python language, enables reading such a format and numerically processing the information contained in it. In the CAM processor implemented for this article, numerical data contained in the mesh were converted into a graphical representation. Following this, the toolpath and the surface's normal vectors within that path were efficiently calculated using algorithms derived from Eulerian graphs and Hamiltonian cycles (Zhang and Guo 1986; Stapleton et al. 2010).

a)

b)

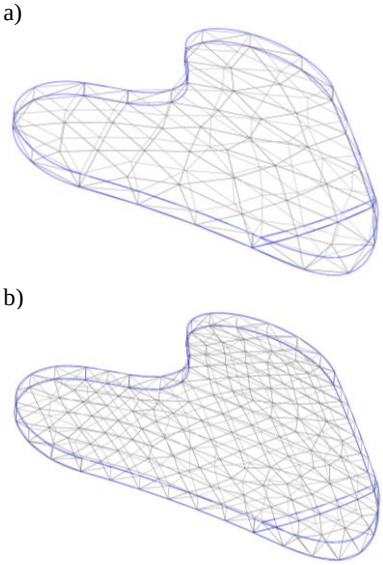

Fig. 1. CAD model with a mesh of (a) low density, (b) high density

Assume that $Q = (Q_1, Q_2, \dots, Q_m)$ represents the path defined by points Q_i between which the tool motion follows a linear trajectory. Therefore, this trajectory consists of a family of straight lines $\Gamma_i(t) = tQ_i + (1-t)Q_{i+1}$. The entire tool motion trajectory Γ can thus be considered as a sequence of individual component trajectories, expressed as $\Gamma = (\Gamma_1, \Gamma_2, \dots, \Gamma_{m-1})$. The first task is to reconstruct normal vectors to the surface on which the path Q is located. While it is not possible to achieve this exactly, we will assume that consecutive points on the path are close enough to each other so that, in the immediate vicinity, the surface can be approximated by a spherical tangent with a specified radius and center.

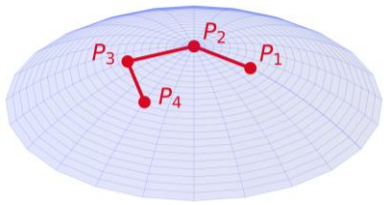

Fig. 2. Example path on a spherical dome

Consider four points $P_1 = (x_1, y_1, z_1)$, $P_2 = (x_2, y_2, z_2)$, $P_3 = (x_3, y_3, z_3)$, and $P_4 = (x_4, y_4, z_4)$ which do not lie in the same plane (Fig. 2). The equation of a sphere with a center at $C = (x_C, y_C, z_C)$ and a radius r is given by equation (1).

$$(X - x_C)^2 + (Y - y_C)^2 + (Z - z_C)^2 = r^2 \quad (1)$$

If we assume that $d = x_C^2 + y_C^2 + z_C^2 - r^2$, then the above equation takes the form of equation (2).

$$X^2 + Y^2 + Z^2 - 2x_C X - 2y_C Y - 2z_C Z + d = 0 \quad (2)$$

The center and radius of the sphere, on which the four previously established points lie, can be explicitly determined. To achieve this, it is necessary to solve a system of linear equations (3).

$$\begin{pmatrix} 2x_1 & 2y_1 & 2z_1 & -1 \\ 2x_2 & 2y_2 & 2z_2 & -1 \\ 2x_3 & 2y_3 & 2z_3 & -1 \\ 2x_4 & 2y_4 & 2z_4 & -1 \end{pmatrix} \begin{pmatrix} x_C \\ y_C \\ z_C \\ d \end{pmatrix} = \begin{pmatrix} x_1^2 + y_1^2 + z_1^2 \\ x_2^2 + y_2^2 + z_2^2 \\ x_3^2 + y_3^2 + z_3^2 \\ x_4^2 + y_4^2 + z_4^2 \end{pmatrix} \quad (3)$$

After finding the solution of linear system (3), the radius of the sphere is determined from the equation $r^2 = x_C^2 + y_C^2 + z_C^2 - d$.

In Fig. 3, a comparison of normal vectors obtained using the method described above (vectors in red) with vectors obtained from the analysis of the surface mesh (vectors in green) is presented. It was observed that when the surface curvature is constant or changes continuously, the reconstructed vectors coincide with

the vectors determined from the surface mesh. However, in the case of a sudden change in curvature, the reconstructed vectors deviate in their direction from the actual normal vectors. In Fig. 3, the discrepancy appears in the bottom right corner, where we encounter a radical change in curvature radius, and the second derivative of the surface function in the direction determined by the trajectory has a discontinuity point.

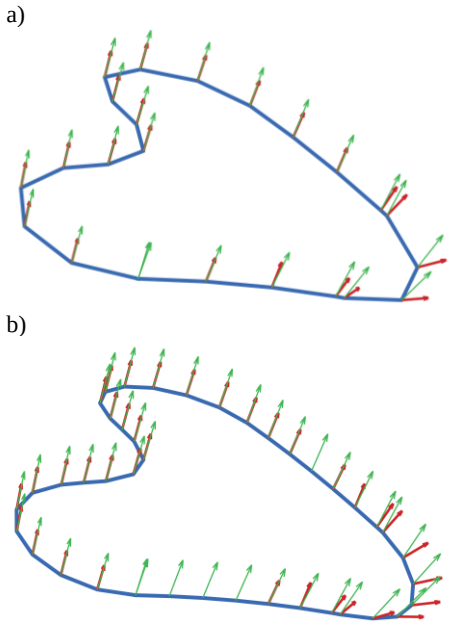

Fig. 3. Normal vectors to the surface obtained from the CAD model (green) and determined based on spherical approximation (red)

The CAD program allows to generate the output path Q with practically any precision. Distances between successive points on the path $|Q_iQ_{i+1}|$ can be so small that the physical movement of the robot between them is practically imperceptible. Considering the finite precision with which the drives of individual robot axes can be adjusted, this results in motion that is not smooth and proceeds much slower than it should. Therefore, the path Q must be adjusted to the physical capabilities of executing movements by a given robot. For each device, there is a minimum size of displacement that it can smoothly perform. Hence, it is necessary to develop a method for selecting from the specified path Q a subset $S \subset Q$ that ensures smooth movements while maintaining the trajectory within a specified tolerance ε.

Now suppose that we have a set of consecutive points on the path $T = (Q_k, Q_{k+1}, \dots, Q_{k+n})$. To determine the error produced by approximating the path T by the segment Q_kQ_{k+n}, it is necessary to determine the maximum value d_j, which is the distance from point Q_j to the segment Q_kQ_{k+n}.

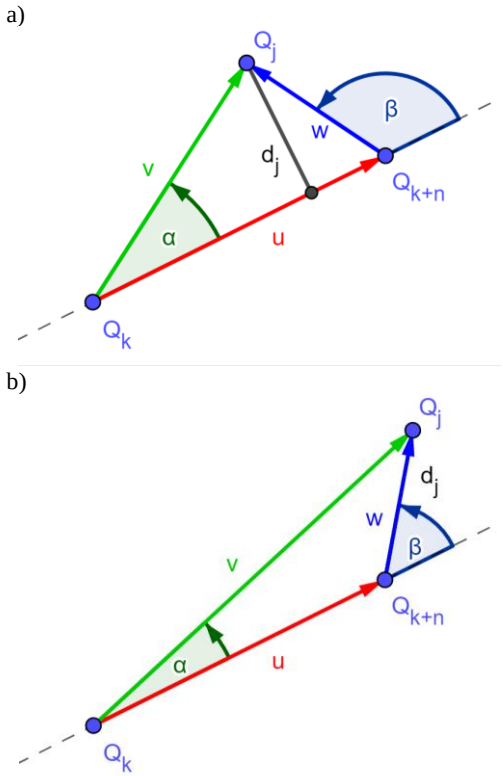

Fig. 4. Distance of point Q_j from segment Q_kQ_{k+n}

To determine the value of d_j, the properties of the cross and dot products can be utilized. In Fig. 4, two situations that may occur are presented. The first situation, illustrated in Fig. 4 (a), occurs when d_j is the distance from point Q_j to the segment Q_kQ_{k+n} – that is, d_j is the height of the triangle $Q_kQ_{k+n}Q_j$. If Q_j does not project onto the segment Q_kQ_{k+n}, as shown in Fig. 4 (b), then the distance d_j is equal to the shorter of the lengths of either side. The resolution of the both cases can be achieved by comparing the signs of the dot products. Case (a) occurs when the dot products $u \cdot v$ and $u \cdot w$ have opposite signs. In comparison, case (b) arises when the signs of both dot products are identical. Using the notations as in Fig. 4, the distance d_j can be expressed by the formula (4).

$$d_j = d(Q_j, Q_kQ_{k+n}) = \\ = \begin{cases} |u \times v|/|u|, & \text{if } (u \cdot v)(u \cdot w) \le 0, \\ \min\{|v|, |w|\}, & \text{if } (u \cdot v)(u \cdot w) > 0. \end{cases} \quad (4)$$

The introduced notations and formulas allow to define an algorithm whose task is to reduce the number of points on the robot's path. This algorithm takes the original path $Q = (Q_1, Q_2, \dots, Q_m)$ and a certain number ε as input arguments, where ε denotes the permissible deviation in determining the new path S for the robot's movement.

Algorithm for optimal path finding

1. read $Q = (Q_1, Q_2, \dots, Q_m)$ and ε;
2. $S \leftarrow (Q_1)$; remove first element from Q;
3. **while** $Q \neq (\ )$ **do**
   a. $T \leftarrow (\ )$;
   b. remove last element of S and append to T;
   c. remove first element of Q and append to T;
   d. **while** $Q \neq (\ )$ **do**
      i. remove first element of Q and append to T;
      ii. assign first element of T as Q_k;
      iii. assign last element of T as Q_{k+n};
      iv. compute $d_{\max} = \max\{d_j\}$, where $d_j = d(Q_j, Q_k Q_{k+n})$ for all Q_j different from Q_k and Q_{k+n};
      v. **if** $d_{\max} > \varepsilon$ **then** break loop 3.d;
   e. **if** $Q \neq (\ )$ **then** remove last element of T and append as first to Q;
   f. remove first element of T and append to S;
   g. remove last element of T and append to S; go to point 3;
4. **return** S;

The effects of the above algorithm were presented in Fig. 5, which shows the path progression for the same target trajectory and different values of permissible deviation.

a)

b)

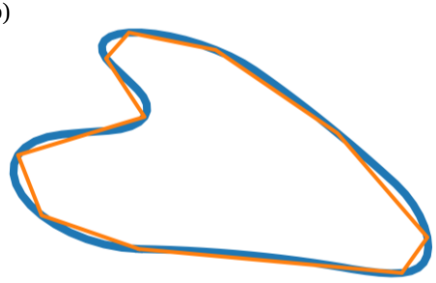

Fig. 5. Example paths (orange) for different values of deviation from the target trajectory (blue)

c)

d)

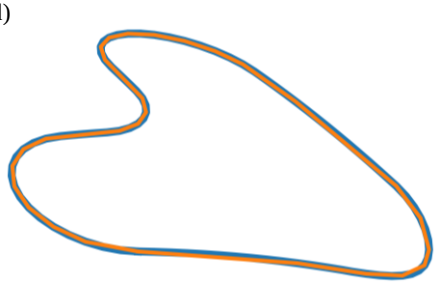

Fig. 5 (cont.). Example paths (orange) for different values of deviation from the target trajectory (blue)

3. Results

For the purposes of the article, CAM software was implemented to transform a MESH file (Gmsh msh version 2.0 ASCII format) into a set of commands that execute the movement of the robot along a given path. The Python language was used for the implementation along with the corresponding mathematical libraries (Chmielowiec 2021; Chmielowiec and Klich 2021). The main element of the created software is the path optimization algorithm presented in the previous section, which adjusts the tool's path of movement based on the size of the permissible deviation from the precise trajectory.

Table 1. Time and velocity of tool movement along a path approximating a circle with a radius of 50 mm using a regular n-sided polygon

		Vertical		Normal to surface	
n	v [mm/s]	t [s]	$\bar{v}$ [mm/s]	t [s]	$\bar{v}$ [mm/s]
6	5	45.2	6.63	45.2	6.64
6	10	22.8	13.18	22.7	13.20
6	20	11.5	25.99	11.6	25.97
6	40	6.0	49.64	6.1	49.45
6	80	3.6	84.01	3.6	84.10
12	5	54.7	5.68	54.9	5.66
12	10	27.6	11.27	27.8	11.17
12	20	14.4	21.64	14.1	22.02
12	40	7.6	40.72	7.6	40.71
12	80	4.9	63.97	5.1	60.61
24	5	59.3	5.29	59.5	5.26
24	10	30.0	10.43	30.0	10.43
24	20	15.7	19.90	15.5	20.19

Table 1 (cont.). Time and velocity of tool movement along a path approximating a circle with a radius of 50 mm using a regular n-sided polygon

		Vertical		Normal to surface	
n	v [mm/s]	t [s]	$\bar{v}$ [mm/s]	t [s]	$\bar{v}$ [mm/s]
24	40	9.1	34.35	9.2	34.16
24	80	6.6	47.49	6.6	47.51
48	5	62.1	5.05	62.1	5.05
48	10	31.7	9.92	31.9	9.84
48	20	16.8	18.64	16.9	18.52
48	40	10.8	29.03	10.9	28.89
48	80	9.9	31.65	10.2	30.72
96	5	63.7	4.93	64.1	4.90
96	10	33.4	9.42	33.5	9.36
96	20	18.6	16.92	18.8	16.68
96	40	13.9	22.67	14.2	22.11
96	80	15.7	19.97	16.0	19.63

The experiments were conducted on a HANWHA HCR-5 robot (Fig. 6), which was equipped with a special holder along with a pen. This made it possible to visually verify the accuracy of the algorithm generating the optimized path.

Fig. 6. Photo of test stand

In the first experiment, the velocity of robot movement was measured as it moved a tool along a path approximating a circle with a radius of 50 mm. The path was parameterized by the number n, which defines the number of vertices of a regular n-sided polygon approximating the circle. Tests were conducted for values of $n \in \{6,12,24,48,96\}$ and nominal velocity $v \in \{5,10,20,40,80\}$ expressed in mm/s. It should be emphasized that by the nominal velocity v, here we refer to the velocity set for the robot as one of the parameters of the motion command. Table 1 lists the times t of the tool's passage along the path and the average velocity of passage $\bar{v}$ when the tool is set vertically and perpendicular to the surface over which it moves. From the numerical data, it is clear that the orientation of the tool does not have a significant impact on the actual velocity of the tool passage along the path. The average relative difference in passage times between these two cases is indeed at the level of 1%. However, a significant change in the velocity of passage can be observed depending on the number of path points n.

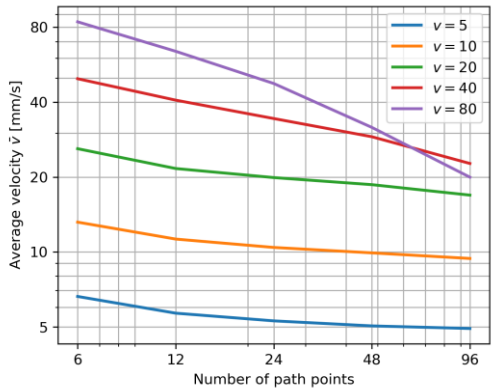

Fig. 7. Average velocity $\bar{v}$ as a function of the number of path points n for different nominal velocity v values

In Fig. 7, one can observe how the average velocity $\bar{v}$ of tool movement clearly decreases with the increasing number of path points. These decreases are significant enough that the use of a logarithmic scale was necessary for the clarity of the plot. Particular attention should be paid to the results obtained for the nominal velocity of $v = 80$ mm/s. The plot clearly shows that the average velocity in the case of a large number of path points drops even below the average velocity obtained for the nominal velocity of $v = 40$ mm/s (the purple curve is below the red for $n = 96$). This result is unexpected and means that in certain cases, it is possible to reduce the passage time of a given path by reducing the nominal velocity.

Table 2. Average time $\bar{t}$ and average valocity $\bar{v}$ of tool movement along shape presented in Fig. 1

			Vertical		Normal to surface	
v [mm/s]	ε [mm]	n	$\bar{t}$ [s]	$\bar{v}$ [mm/s]	$\bar{t}$ [s]	$\bar{v}$ [mm/s]
80	0.1	60	11.2	25.63	11.2	25.59
80	0.2	42	9.0	31.61	8.8	32.31
80	0.5	26	6.7	42.41	6.7	42.26
80	1.0	18	5.7	49.38	5.9	48.32
80	2.0	14	5.2	54.00	5.2	53.98

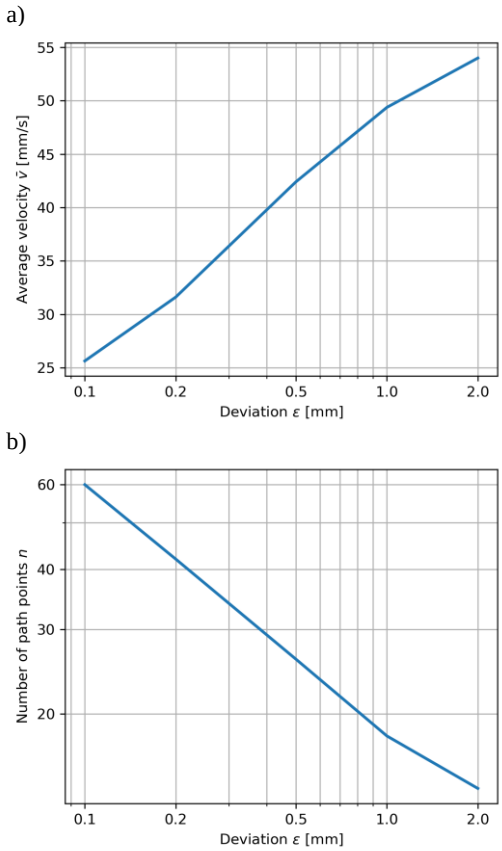

Fig. 8. Average valocity $\bar{v}$ as a function of: deviation ε (a), number of path points n generated by the algorithm as a function of deviation ε (b)

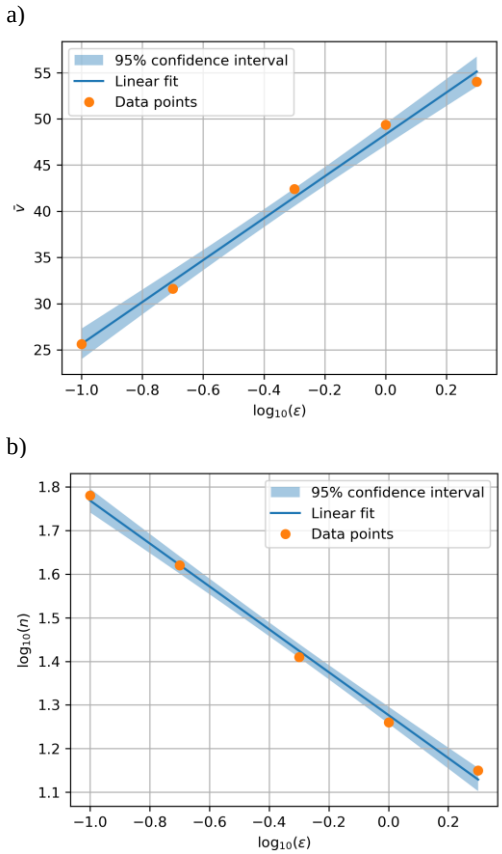

Fig. 9. Linear approximation of average velocity $\bar{v}$ as a function of: deviation logarithm $\log_{10}\varepsilon$ (a), linear approximation of path points number logarithm $\log_{10}n$ generated by the algorithm as a function of deviation logarithm $\log_{10}\varepsilon$ (b)

Subsequent measurements were conducted for the shape presented in Fig. 1. A path generation algorithm was used to generate motion instructions for the robot, whose tool would move along the specified trajectory with various values of deviation ε. For each selected value of ε, 5 measurements were conducted at a fixed nominal valocity of $v = 80$ mm/s. The average values of the obtained results have been presented in Table 2. In Fig. 8 the relationships between the adopted value of permissible deviation ε, and the average valocity of traversal along the path (Fig. 8 (a)) and the number of path points (Fig. 8 (b)) are presented.

The use of logarithmic scale for the ε and n axes shows linear relationships between the values obtained during the measurements. Using the method of least squares, the following relationships can be obtained for the studied intervals:

$$\bar{v} = 22.66 \cdot \log_{10}(\varepsilon) + 48.31 \tag{5}$$

$$\log_{10}(n) = -0.50 \cdot \log_{10}(\varepsilon) + 1.28 \tag{6}$$

Both relationships are graphically presented in Fig. 9 (a) and Fig. 9 (b), along with the marked set of measurement data and the confidence interval for the least squares method.

4. Summary

In this article, an algorithm is presented that allows to generate the robot's motion path based on data from a CAD model. The algorithm operates based on the precise trajectory of the tool and the deviation value ε, which defines the deviation of the generated path from the original trajectory. This algorithm is a greedy type of algorithm and has been implemented in a CAM processor prepared for the purposes of this article. The created tool was used to conduct experiments on an actual HANWHA HCR-5 collaborative robot. The tests showed that defining too high a nominal velocity in the robot's motion instructions can have the opposite effect to the intended one, and cause the traversal of a given path to slow down even compared to a lower nominal velocity. The obtained results clearly show that the best way to maintain an appropriate velocity of robot movement is to adjust the number of path points to the given nominal velocity. However, it should be remembered that too large number of path points significantly reduces the efficiency of robot movements and lowers the average velocity of passage. The relationship $\log_{10}(n) = -0.50 \cdot \log_{10}(\varepsilon) + 1.28$ derived from simulation

data can be simplified to the equation $\varepsilon = \frac{363}{n^2}$, which demonstrates the effectiveness of the presented algorithm. It implies that doubling the number of points results in a fourfold reduction in deviation from the desired trajectory. Despite this, it is worth analyzing other methods for generating and optimizing the robot's motion path in order to achieve the smallest possible number of points for a given motion precision.

The methods presented in the article can be applied in processes such as burning, milling, and applying adhesives and sealants.. The automation of these processes using collaborative robots is currently quite limited by the lack of suitable software tools for automatically generating robot instructions. The approach introduced allows for efficient and precise application of assembly adhesives and various types of sealants. It also enables cutting of various patterns on surfaces of practically any shape, which, at a later stage of production, allows for the assembly and attachment of other elements.

References

Abd Rahman, Z., Mohamed, S.B., Minhat, M., & Abd Rahman, Z. (2023). "Design and Development of 3-Axis Benchtop CNC Milling Machine for Educational Purpose." *International Journal of Integrated Engineering* 15 (1): 145–60. https://doi.org/10.30880/ijie.2023.15.01.013.

Ali, S. M., & Mohsin, H. (2021). "Design and Fabrication of 3-Axes Mini CNC Milling Machine." *IOP Conference Series: Materials Science and Engineering* 1094 (1): 012005. https://doi.org/10.1088/1757-899X/1094/1/012005.

Berx, N., Decré, W., & Pintelon, L. (2024). "A Tool to Evaluate Industrial Cobot Safety Readiness from a System-Wide Perspective: An Empirical Validation." *Safety Science* 170: 106380. https://doi.org/10.1016/j.ssci.2023.106380.

Chmielowiec, A. (2021). "Algorithm for error-free determination of the variance of all contiguous subsequences and fixed-length contiguous subsequences for a sequence of industrial measurement data." *Computational Statistics* 36 (4): 2813–40. https://doi.org/10.1007/s00180-021-01096-1.

Chmielowiec, A., & Klich, L. (2021). "Application of python libraries for variance, normal distribution and Weibull distribution analysis in diagnosing and operating production systems." *Diagnostyka* 22 (4): 89–105. https://doi.org/10.29354/diag/144479.

Chutima, P. (2023). "Assembly Line Balancing with Cobots: An Extensive Review and Critiques." *International Journal of Industrial Engineering Computations* 14 (4): 785–804. https://doi.org/10.5267/j.ijiec.2023.7.001.

Da Silva, M., Regnier, R., Makarov, M., Avrin, G., & Dumur, D. (2023). "Evaluation of Intelligent Collaborative Robots: A Review." In *2023 IEEE/SICE International Symposium on System Integration (SII)*, 1–7. IEEE. https://doi.org/10.1109/SII55687.2023.10039365.

Faulwasser, T., Weber, T., Zometa, P., & Findeisen, R. (2016). "Implementation of Nonlinear Model Predictive Path-Following Control for an Industrial Robot." *IEEE Transactions on Control Systems Technology* 25 (4): 1505–11. https://doi.org/10.1109/TCST.2016.2601624.

Gayathri, N., Sundar, M., Sargurunathan, R., Sudharsan, R., & Sajith, A.. (2022). "Design of Voice Controlled Multifunctional Computer Numerical Control (CNC) Machine." In *2022 International Conference on Inventive Computation Technologies (ICICT)*, 657–63. https://doi.org/10.1109/ICICT54344.2022.9850659.

Geuzaine, C., & Remacle, J.-F. (2009). "Gmsh: A 3-D finite element mesh generator with built-in pre-and post-processing facilities." *International Journal for Numerical Methods in Engineering* 79 (11): 1309–31. https://doi.org/10.1002/nme.2579.

Hu, M. (2023). "Research on Safety Design and Optimization of Collaborative Robots." *International Journal of Intelligent Robotics and Applications* 7 (4): 795–809. https://doi.org/10.1007/s41315-023-00299-7.

Jocelyn, S., Ledoux, E., Marrero, I.A., Burlet-Vienney, D., Chinniah, Y., Bonev, I.A., Mosbah, A.B., & Berger, I. (2023). "Classification of Collaborative Applications and Key Variability Factors to Support the First Step of Risk Assessment When Integrating Cobots." *Safety Science* 166: 106219. https://doi.org/10.1016/j.ssci.2023.106219.

Khan, A., Shukla, A.K., & Singh, A. (2018). "Design and Fabrication of 3-Axis Computer Numerical Control (CNC) Milling Machine." *International Journal of Creative Research Thoughts* 6 (2): 1347–53.

Kheirabadi, M., Keivanpour, S., Chinniah, Y.A., & Frayret, Y.-M. (2023). "Human-Robot Collaboration in Assembly Line Balancing Problems: Review and Research Gaps." *Computers & Industrial Engineering* 186: 109737. https://doi.org/10.1016/j.cie.2023.109737.

Khoramshahi, M., & Billard, A. (2019). "A Dynamical System Approach to Task-Adaptation in Physical Human–Robot Interaction." *Autonomous Robots* 43: 927–46. https://doi.org/10.1007/s10514-018-9764-z.

Lin, R.-S. (2000). "Real-time surface interpolator for 3-D parametric surface machining on 3-axis machine tools." *International Journal of Machine Tools and Manufacture* 40 (10): 1513–26. https://doi.org/10.1016/S0890-6955(00)00002-X.

Matheson, E., Minto, R., Zampieri, E.G.G., Faccio, M., & Rosati, G. (2019). "Human–Robot Collaboration in Manufacturing Applications: A Review." *Robotics* 8 (4). https://doi.org/10.3390/robotics8040100.

Nagata, F., Yoshitake, S., Otsuka, A., Watanabe, K., & Habib, M.K. (2013). "Development of CAM System Based on Industrial Robotic Servo Controller Without Using Robot Language." *Robotics and Computer-Integrated Manufacturing* 29 (2): 454–62. https://doi.org/10.1016/j.rcim.2012.09.015.

Parsa, S., & Saadat, M. (2021). "Human-Robot Collaboration Disassembly Planning for End-of-Life Product Disassembly Process." *Robotics and Computer-Integrated Manufacturing* 71: 102170. https://doi.org/10.1016/j.rcim.2021.102170.

Stapleton, G., Rodgers, P., Howse, J., & Zhang, L. (2010). "Inductively generating Euler diagrams." *IEEE Tran-*

sactions on Visualization and Computer Graphics 17 (1): 88–100. https://doi.org/10.1109/TVCG.2010.28.

Suh, S.-H., Kang, S.K., Chung, D.-H., & Stroud, I. (2008). *Theory and Design of CNC Systems*. Springer Science & Business Media. https://doi.org/10.1007/978-1-84800-336-1.

Toledano-García, A.A., Pérez-Cabrera, H.R., Ortega-Cabrera, D., Navarro-Durán, D., & Pérez-Hernández, E.M. (2023). "Trajectory Generator System for a UR5 Collaborative Robot in 2D and 3D Surfaces." *Machines* 11 (9). https://doi.org/10.3390/machines11090916.

Weidemann, C., Mandischer, N., van Kerkom, F., Corves, B., Hüsing, M., Kraus, T., & Garus, C. (2023). "Literature Review on Recent Trends and Perspectives of Collaborative Robotics in Work 4.0." *Robotics* 12 (3). https://doi.org/10.3390/robotics12030084.

Zhang, F.-J., & Guo, X.-F. (1986). "Hamilton cycles in Euler tour graph." *Journal of Combinatorial Theory, Series B* 40 (1): 1–8. https://doi.org/10.1016/0095-8956(86)90060-2.